AL.2.1989-354

APPENDIX 22

SYSTEMATIC ASSESSMENT OF PROTECTIVE CLOTHING FOR ALBERTA WORKERS

A PROJECT FUNDED BY THE
OCCUPATIONAL HEALTH AND SAFETY
HERITAGE GRANT PROGRAM

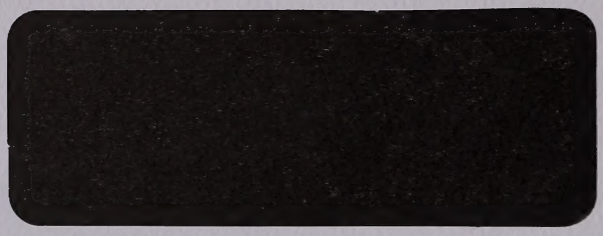

CANADIANA
C2
AUG 2 9 1989

APPENDIX 22

SYSTEMATIC ASSESSMENT OF PROTECTIVE CLOTHING FOR ALBERTA WORKERS

SYSTEMATIC ASSESSMENT 0F PROTECTIVE CLOTHING FOR ALBERTA WORKERS

Final Research Project Report
Prepared for
Alberta Occupational Health and Safety
Heritage Grant Program

by

E.M. Crown, K.B. Rigakis and J.D. Dale

June 15, 1989

APPENDIX 22

Digitized by the Internet Archive
in 2015

https://archive.org/details/systematicassess01crow

APPENDIX 22

A LITERATURE REVIEW OF THERMAL INJURY

by

E.Y. Leung

Department of Mechanical Engineering
University of Alberta
Edmonton, Alberta, Canada

March, 1988

ABSTRACT

The objectives of the present report are to understand thermal injury and to provide methods for evaluation of skin damage due to thermal exposures. This report reviews the literature of thermal injury for the period from the late 1940's to the 1970's. Examination of the literature into the 1980's found that the quantification of thermal injury is still based on the earlier work. This report covers a mathematical and experimental analysis of heat transfer to the skin, the studies of thermal properties of the skin and its physiological reactions to burns. Methods to estimate skin damage incurred during a burn were also included.

TABLE OF CONTENTS

	Page
1. Introduction	1
2. The Human Skin	3
2.1 The Structure of Skin	3
2.2 The Thickness of Skin	6
3. Change of Skin Temperature in Response to Various Conditions of Heat Exposure	10
3.1 Mathematical Deductions	10
3.1.1 Hot Surrounding Medium	11
3.1.2 Direct Thermal Contact	12
3.1.3 Nonpenetrating Heat Flow	13
3.1.3.1 Constant Heat Flow	13
3.1.3.2 Square-Wave Pulse of Heat Flow	13
3.1.4 Penetrating Radiant Heat	14
3.2 Analysis of Theoretical and Experimental Results	17
4. The Thermal Properties of Skin	21
5. The Quantitative, Qualitative and Sensational Effects of Heat on the Skin	28
5.1 General Consideration of the Quantitative and Qualitative Effects	28
5.2 General Consideration of the Sensational Effect	31
5.3 Thresholds of Burns, Blistering and Pain as Related to the Intensity and Duration of Thermal Exposure	33
5.4 Factors Affecting the Effects of Thermal Exposure on the Skin	40
6. Prediction of Cumulative Tissue Damage Incurred During a Burn and Its Relation to Pain Intensity	44
7. Computer Models to Determine the Thermal Injury from Experimental Data	52
8. Summary	62
References	64

LIST OF FIGURES

		Page
1.	The Epidermis	4
2.	The Dermis	4
3.	Temperature Rises at Different Skin Layers Due to a Direct Contact Exposure	15
4.	Temperature Rises at Different Skin Layers Due to a Nonpenetrating Constant Heat Exposure	16
5.	Temperature-Time History of Skin Exposed to a Square-Wave Pulse of Nonpenetrating Radiation	16
6.	Increase of Skin Surface Temperature with Time During a Penetrating Radiation Exposure	17
7.	Surface Temperature of Human Forearm With and Without Blood Flow Obstruction When Exposed to a Radiation of 0.055 cal/cm^2 sec	20
8.	Variations of the Thermal Conductivity of Human Skin with Tissue Temperature at 80 μm deep	27
9.	Pain Intensity Induced by Heating the Forehead and Forearm for a Duration of 3 Seconds	33
10.	Time-Surface Temperature Thresholds at Which Cutaneous Burning Occurs	35
11.	Human Skin Tolerance Time to Absorbed Thermal Energy	37
12.	Relationship Between Pain Intensity and Skin Surface Temperature Obtained by Heating the Surface of the Forehead	39
13.	The Damage Rate Against the Tissue Temperature at 80 μm Such that $\Omega = 1$ at Threshold Blistering	48
14.	Correlation of Pain Intensity with Damage Rate and Tissue Temperature at 80 μm	50
15.	Temperatures at the Surface and those Calculated at 80 μm During Heating and Cooling of the Skin by Thermal Radiation	53
16.	Damage Rate Versus the Time at Which the Basal Layer Temperature Occurred	54
17.	Experimental and Theoretical Thermal Conductivity of Skin Versus Tissue Temperature	57

List of Figures Continued

		Page
18.	Experimental and Theoretical Time-Temperature History at the Basal Layer for an Irradiance of 0.4 cal/cm^2 sec	57
19.	Reciprocal of τ versus Radiation Level	59
20.	Thermal Conductivity versus Radiaton Level	59

LIST OF TABLES

		Page
1.	Weighting of Areas with Respect to Total Skin Surface	3
2.	The Thickness of the Epidermis in μm	7
3.	The Thickness of the Dermis in μm	8
4.	The Computed Time-Temperature Relationships at the Basal Layer when an Entire Animal (~ 30 cm diameter) is Surrounded by an Envelope of Ambient Air and Radiant Heat with a Constant Temperature Source	18
5.	The Computed Time-Temperature Relationships at the Basal Layer When the Skin Surface is Immediately Brought to and Maintined at, a Specific Temperature	18
6.	The Measured Time-Temperature Relationships for the Dermal-Fat Interface when the Skin Surface is Immediately Brought to, and Maintained at a Specific Temperature	19
7.	Thermal Conductivity (k), Capacity (c) and Density (ρ) of Cutaneous and Subcutaneous Tissues	22
8.	Thermal Diffusivity ($k/\rho c$) and Conductivity (k) of Different Skin Layers	23
9.	Thermal Inertia ($k\rho c$) of Human Tissues	25
10.	Thermal Inertia ($k\rho c$) of Skin at Pain Threshold	25
11.	Stimulus Intensity, Exposure Time and Skin Surface Temperature at Pain Threshold	39
12.	The Cumulative Effects of Repeated Subthreshold Thermal Exposures on Porcine Skin	42
13.	Relationship Between Pain, Tissue Temperature and Damage Rate	51
14.	Characteristics of Time-Temperature Histories of Skin Exposed to Thermal Radiation Just Sufficient to Cause Minimal Blistering	60

1. INTRODUCTION

Thermal injury was a major source of morbidity and mortality during World War II. Since that time, attentions have been paid to the studies of skin damage due to thermal exposure in order to develop protective devices and to give medical care to the military. Consequently, numerous reports on this topic appeared. Today, statistics indicate that thermal injury is one of the major types of trauma in the modern society. Thermal injury frequently occurs at industrial sites where the risk of fires is high. Burns from clothing fires also occur most often in the home.

One method to minimize burn injury is to use heat resistant fabrics for safety apparel. Instrumented mannikins are usually employed in experiments to evaluate protective clothing. From the measurements of heat transfer through fabrics to the mannikin, the severity of burns can be assessed by means of the available knowledge regarding the relationship between the heat transfer and its resultant skin damage.

Thermal damage to the skin occurs as a result of an increase in tissue temperature above an injurious level within a finite period of time. The severity of burns depends on the intensity and duration of exposures. The mode of heat transfer can be conduction, convection, radiation, or any combination of the above mechanisms.

To understand the problem of thermal injury and to provide adequate information for assessment of skin damage due to thermal exposure through the use of an instrumented mannikin, the present report reviews the literature of thermal injury. The pioneering works of many investigators (around 1950 to 1970) will be presented. A mathematical and physical analysis of the physiological response of skin to burns will be covered.

Chapter 2 briefly describes the anatomy of human skin. Chapter 3 illustrates the response of skin temperature to various conditions of heat exposure. Mathematical expressions describing the change of skin temperature under different conditions are deduced. The thermal properties of the skin are discussed in Chapter 4. The variations of these properties with layer, site, moisture content, irradiation and temperature are explained. In Chapter 5, the quantitative, qualitative and sensational effects of heat on the skin are studied. Information concerning the thresholds of burns, blistering and pain as related to the intensity and durations of thermal exposure is given. Factors that may alter the vulnerability of skin to thermal injury are also discussed. Chapter 6 summarizes the physical and chemical processes that participate in cell death during a burn. A rate process model is developed in this chapter to predict the skin damage. Relationship between pain intensity and skin damage is shown. Chapter 7 demonstrates some of the numerical procedures that are available for determination of the severity of burns from experimental data using digital computers. This is followed by a brief summary of the review in Chapter 8.

2. THE HUMAN SKIN

The skin covers the entire body and is, therefore, as large as the body itself. For most adults, the area is about 1.6 to 1.9 square meters [1]. Table 1 shows the weighting of area for each portion of the body [2]. The functions of the skin are diverse and include protection, excretion, sensation, maintaining fluid and electrolyte balance and body temperature.

TABLE 1
Weighting of Areas with Respect to Total Skin Surface,
From Stoll and Chianta [2]

	% of Total Area
Head	7
Trunk	35
Arms	14
Hands	5
Thighs	19
Legs	13
Feet	7

2.1 The Structure of Skin

The skin is made up of two main layers: an outer layer, the epidermis, and an inner layer, the dermis or corium. The tissues under the skin, such as the fatty tissue and muscle, are called the subcutaneous or hypodermic tissues. The tissues within the layers of the skin are called the intracutaneous or cutaneous tissues. The structures of the epidermis and the dermis are depicted in Figures 1 and 2, respectively.

The epidermis consists of squamous epithelial tissue and is divided into characteristic strata (Figure 1). The stratum germinativum or the basal layer is the deepest stratum from which new cells are produced. The cells move upward as they form and gradually flatten. In the stratum granulosum, the cells die and their nuclei degenerate. The dead cells are converted into a tough fibrous protein called keratin which is water-

Figure 1 The Epidermis, from Gardner and Osburn [3]

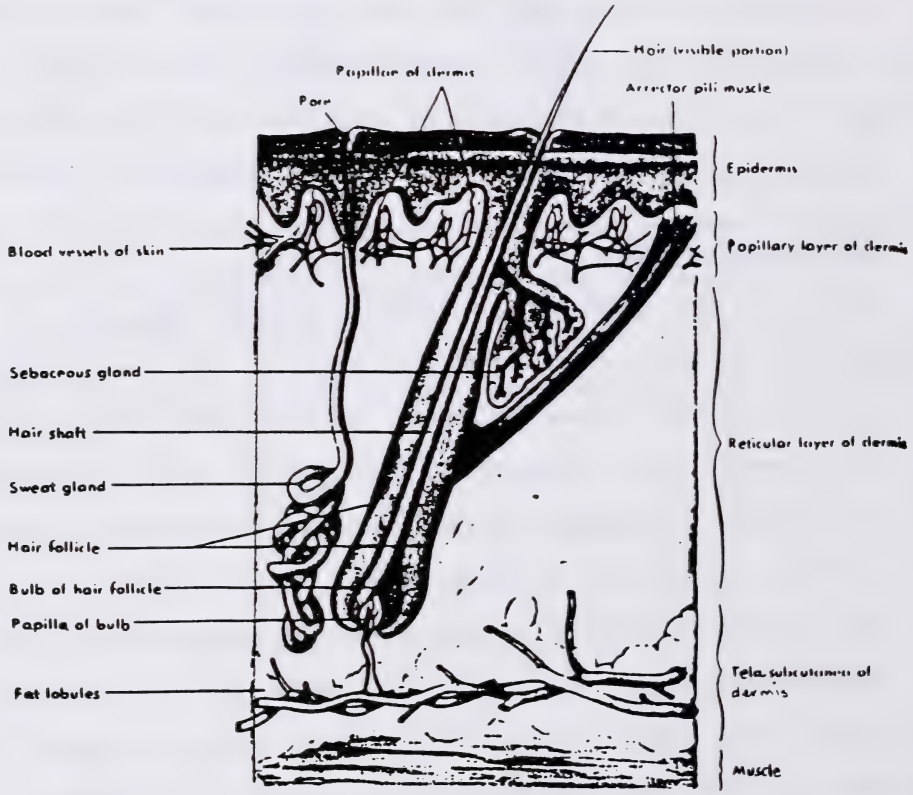

Figure 2 The Dermis, from Gardner and Osburn [3]

repellant and resistant to abrasion. The keratin is formed in the stratum corneum (the horny layer) in which the new keratin keeps pushing upward to replace the old ones that continually flake off from the skin surface.

The dermis is composed of fibrous connective tissue which provides strength and elasticity for the skin (Figure 2). The glands of the skin, the hair follicles, and the blood vessels are all located within this layer. The dermis is further divided into a superficial papillary layer and a deeper reticular layer. The papillary layer presses against the epidermis so that the blood vessels in the papillary layer are in close contact with the epidermis. As a result, nutriments and oxygen reach the epidermis by diffusion. The papillary layer is also thrown up into papillary ridges, especially in the fingers, palms and soles. These ridges, covered with epidermis, form an unique pattern on the skin surface in each individual. These patterns of the ridges are known as finger prints, palm prints or sole prints.

The root of the hair is embedded in the reticular layer. Together with its coverings (a continuation of the stratum germinativum), the root forms the hair follicle. At the bottom of the follicle is a loop of capillaries enclosed in a connective tissue papilla. The epithelial cells over the papilla reproduce and undergo keratinization (a process of keratin formation) to form the hair shaft. A small band of involuntary muscle fibers, the arrector pili, connects the hair follicle to the papillary layer. When these muscles contract in response to cold or fright, they pull the hair erect. As a result, the skin around the hair is raised and goose pimples are formed. Two or more sebaceous glands cluster beside each

hair follicle. These glands secrete an oily product, sebum, to keep the hairs soft and pliable.

Sweat glands are long tubular glands. The coiled secretory portions of the glands are located in the reticular layer or even in the subcutaneous layer. Sweat secretion eliminates water from the body to maintain fluid and electrolyte balance and body temperature.

Millions of sensory receptors are distributed throughout the skin. These receptors are the distal ends of dendrites of all sensory nerve cells (neurons). The simplest receptors are merely the free endings of sensory dendrites. They are mainly in the dermis. Some of them surround the root of the hair follicle in linear and circular fashion, and some extend to the epidermis. The free nerve endings are those which mediate touch, coldness, hotness and pain such as that caused by thermal injury. A more complete description of the structure of the skin and its sensory organ is in References [1] and [3].

2.2 The Thickness of Skin

Unlike the skin structure, the thickness of the skin varies considerably with age, sex, race and site. Southwood [4] studied the variations of the thickness of both epidermis and dermis in various regions from both sexes and at different ages. He commented that the thickness of the epidermis was inversely proportional to the hair density. Thus the areas with the thickest epidermis were those having no hairs, for example: the palms and the soles. In his paper, the only comment on the difference in skin thickness between races is that the epidermis of Negro was thicker than that of the European. His results are shown in Tables 2 and 3.

Table 2 The Thickness of the Epidermis in μm, from Southwood [4]

	Sex	Age														
		0–5	6–10	11–15	16–20	21–25	26–30	31–35	36–40	41–45	46–50	51–55	56–60	61–65	66–70
Medial thigh	M	*27*		*84*	*54*		*71*	*53*	*62*		*60*	*61*		*57*	*39*
	F	50			44		18		55		46	38	39	34	40
Lat. thigh	M	*27*		*83*	*69*		*78*	*60*	*39*		*70*	*69*		*43*	*37*
	F	44			46		63		55		48	45	51	47	35
Post. thigh	M			*86*	*74*		*91*	*58*	*37*		*59*	*54*		*45*	*33*
	F	56					35		48		58	60	51	53	43
Medial leg	M	*23*		*69*	*53*		*52*	*49*	*55*	*38*	*53*	*51*		*51*	*38*
	F	52			53		35		113		57	48	47	48	49
Lat. leg	M	*73*		*80*	*73*		*78*	*61*	*60*	*55*	*72*	*69*		*53*	*42*
	F	48			52		39		40		56	51	51	53	55
Post. leg	M	*24*		*77*	*70*		*80*	*63*	*47*	*57*	*57*	*58*		*55*	*37*
	F	43					39		57		59	52	49	69	36
Sole	M				*864*			*940*	*1061*		*1170*	*1377*		*1282*	*529*
	F				619				850		1094	1020	944	707	
Ant. Abd.	M	*25*		*61*	*42*		*49*	*46*	*39*		*34*	*45*		*38*	*31*
	F	41			37		34		42		46	41	37	47	33
Ant. Thor.	M	*67*		*56*	*48*		*62*	*41*	*68*		*39*	*40*		*35*	32
	F	38			35		26		47		46	42	25	38	
Axilla	M				*46*			*43*	*44*		*43*				
	F	39			75						51			45	
Back	M	*22*		*67*	*58*		*85*	*63*	*92*		*49*	*60*		*60*	
	F	46					45		61		56	49	47	47	44
Pubis	M				*55*			*48*	*48*		*42*				
	F	37			47						43				
Med. arm	M			*59*	*42*		*45*	*37*	*52*		*49*	*61*		*38*	34
	F	41			40				36		42	43	34	53	30
Lat. arm	M	*23*		*67*	*59*		*71*	*46*	*41*		*48*	*49*		*39*	35
	F	44			46		40		54		53	51	47	42	46
Back forearm	M				*60*			*49*	*65*		*49*	*59*		*58*	37
	F	53			50						53	55	55	50	
Front forearm	M	*29*		*79*	*63*		*65*	*66*	*34*		*64*	*57*		*68*	38
	F	44			41		39		59		61	59	53	52	46
Finger	M				*673*		*567*	*420*	*673*		*432*			*533*	580
	F	384			395				539		413	384	539	503	
Face	M								*52*						

(The figures printed in italics represent skin taken from males.)

Table 3 The Thickness of the Dermis in μm, from Southwood [4]

	Sex	Age												
		0–5	6–10	11–15	16–20	21–25	26–30	31–35	36–40	41–45	46–50	51–55	56–60	61–65	66–70
Medial thigh	M	*636*		*576*	*1083*		*1258*	*1312*	*1296*		*1161*	*1125*		*1037*	*1027*
	F	510			845		1071		978		941	877	833	841	796
Lat. thigh	M	*561*		*638*	*1226*		*1802*	*1547*	*1637*		*1161*	*1472*		*1284*	*1199*
	F	814			996		1367		1229		1351	1314	949	913	851
Post. thigh	M			*1056*	*1278*		*1314*	*1168*	*1217*		*1071*	*1101*		*1020*	*1015*
	F	863					1088		1017		1102	1071	1153	1176	1180
Medial leg	M	*527*		*913*	*957*		*1654*	*1151*	*1887*	*857*	*967*	*1122*		*879*	*1187*
	F	828			578		816		757		706	714	694	622	505
Lat. leg	M	*440*		*913*	*1376*		*1573*	*1136*	*1683*	*1217*	*925*	*1115*		*1037*	*1095*
	F	692			802		634		694		741	1005	865	758	530
Post. leg	M	*606*		*636*	*1404*		*1672*	*1365*	*1173*	*1081*	*1209*	*984*		*1029*	*901*
	F	532					1071		847		826	833	731	865	638
Sole	M				*996*				*1805*		*1263*	*1595*			
	F				807				1535					1561	
Ant. Abd.	M	*575*		*1020*	*1741*		*2015*	*1933*	*2584*		*1741*	*1862*		*1671*	*1345*
	F	710			1195		1088		1289		1174	1404	1491	1516	1008
Ant. Thor.	M	*536*		*655*	*1418*		*1683*	*1960*	*1762*		*1592*	*1499*		*1394*	*1363*
	F	860			1307		867		1532		1261	1224	1083	1027	
Axilla.	M				*1230*			*1296*	*1188*		*1076*				
	F	466			1202						1091			1006	
Back	M	*527*		*1102*	*2468*		*2169*	*2492*	*2193*		*2597*	*2300*		*1972*	
	F	840					1930		1535		1456	1583	1559	1666	2242
Pubis	M				*826*			*969*	*1107*		*921*				
	F	932			859						867				
Med. Arm	M			*658*	*856*		*1276*	*1246*			*1173*	*1190*		*1103*	*974*
	F	510			615				796		727	743	689	645	563
Lat. Arm	M	*464*		*806*	*1314*		*1450*	*1843*	*1941*		*1284*	*1522*		*1301*	*1029*
	F	901			961		1097		1252		996	918	672	974	1224
Back Forearm	M				*1197*			*1254*	*1020*		*1013*	*1018*		*972*	*852*
	F	935			1071						827	833	706	681	
Front Forearm	M	*661*		*551*	*1042*		*1107*	*1148*	*1248*		*976*	*1043*		*1003*	*940*
	F	757			850		918		845		812	774	668	689	692
Finger	M										*1207*			*1200*	
	F								1326			894			
Face	M								*1271*						*1411*

(The figures printed in italics represent skin taken from males.)

As shown, men have thicker dermis than women. The epidermis is thickest in the sole. But the dermis is thickest in the trunk. At birth and during childhood, the epidermis is relatively thin. It becomes thicker at about puberty and maintains this thickness until 50 to 60 years old. Then it becomes thinner again. However, the thickness of the dermis increases with age to a maximum at about 30 to 40 years old and subsequently decreases. In general, the thickness of the epidermis and dermis ranges from 20 to 1400 μm and 400 to 2500 μm, respectively.

3. CHANGE OF SKIN TEMPERATURE IN RESPONSE TO VARIOUS CONDITIONS OF HEAT EXPOSURE

When a body is exposed to a heat flux, the temperature of the skin increases. If the heat flux is intense enough to raise the skin temperature beyond a safety limit within a period of time, thermal injury (cutaneous burn) occurs. To prevent the occurrence of thermal injury by protective devices, a knowledge of the responses of skin temperature to different kinds of heat applications is essential. In the past, mathematical expressions have been formulated to describe the relationships between the heat transfers and the skin temperature changes. Experimental results of the responses of skin temperature to different kinds of exposure have also been determined.

3.1 Mathematical Deductions

Although there are numerous complex factors that are involved in the transfer of heat to and through the skin such as variations of skin thickness, existing temperature gradients within the skin, blood flow rate through the various skin layers, density, heat capacity and thermal conductivity of the different layers, Henriques and Moritz [5] mentioned that it was possible to derive a first approximation of the time-temperature relationship in the basal epidermal layer or within the epidermis. Buettner [6] summarized the mathematical deductions for various conditions of heat exposure, including a hot surrounding medium, direct thermal contact, non-penetrating radiant heat, penetrating heat, and others.

They considered the skin as a solid with a plane, infinite boundary and assumed its material properties to be independent of depth. Then the

solutions can be obtained from the energy balance equation of a skin element which is simply the common differential equation of heat conduction:

$$\frac{\partial T}{\partial t} = \alpha \frac{\partial^2 T}{\partial x^2} \tag{1}$$

where T = temperature, °C
t = time, sec.
x = distance below the surface, cm
$\alpha = k/\rho c$ = diffusivity, cm^2/sec
k = heat conductivity, cal/cm sec °C
ρ = density, g/cm^3
C = specific heat capacity, cal/g °C

Equation (1) can be solved by many methods such as Fourier Integral, Laplace Transformation and similarity solution, provided that the boundary and initial conditions are known [7, 8, 9].

3.1.1 Hot Surrounding Medium

In this case, the body is surrounded completely by an envelope of ambient hot fluid (e.g. warm air). Assuming a zero temperature gradient within the skin at $t = 0$, the initial and boundary conditions are:

$$t = 0, \quad x \geq 0, \quad T = T_o \tag{2}$$

$$t > 0, \quad x = 0, \quad -k \frac{dT}{dx} = h(T_a - T_s) \tag{3}$$

Then the temperature T at depth x and time t by solving Eqs. (1), (2) and (3) is:

$$\frac{T_a - T}{T_a - T_o} = \operatorname{erf}\left(\frac{x}{2\sqrt{\alpha t}}\right) + e^{(\alpha h^2 t/k^2 + hx/k)} \left[\operatorname{erfc}\left(\frac{x}{2\sqrt{\alpha t}} + \frac{h\sqrt{\alpha t}}{k}\right)\right] \tag{4}$$

where T_o = initial skin temperature, °C
T_a = ambient temperature, °C
T_s = skin surface temperature, °C
h = heat transfer coefficient between the skin surface and the surroundings, $cal/cm^2.sec.°C$

$\text{erf}(u) = \frac{2}{\sqrt{\pi}} \int_o^u e^{-y^2} dy$ = Error Function

erfc (u) = 1 - erf(u) = complementary Error Function

u = upper limit of the Integral of the Error Function

y = dummy variable

The results of the Error Function for different values of u are tabulated in p. 495 of Reference [8]. The heat transfer coefficient, h, depends on the transfer mechanisms. Equations that describe the heat transfers by convecton (q_c) and radiation (q_r) have been given in [5]. These equations are:

$$q_c = 0.0026 \ (T_a - T_s)^{1.25} \tag{5}$$

$$q_r = 6.56 \times 10^{-11} \ (T_r^4 - T_s^4) \tag{6}$$

Equation (5) is the convection transfer due to an air stream with a velocity of about 1.6 km/hr to a cylindrical object of about 30 cm in diameter, where q_c is in cal/min.cm^2, T_a and T_s are in °C. Equation (6) is the radiation transfer, in cal/min.cm^2, to a body of temperature T_s, in K, completely enclosed in a large box of temperature T_r, in K.

The heat transfer coefficient, h, for both convection and radiation can be obtained by combining the contributions of convection and radiation to heat transfer coefficient as computed by Eqs. (5) and (6).

3.1.2 Direct Thermal Contact

When heat transfer occurs between the skin and a hot body by contact, e.g. boiling water, the skin surface is brought immediately to, and maintained at a constant temperature equal to the hot body temperature. In this case, the heat transfer coefficient, h, is almost infinite, and the boundary condition is:

$$t > 0, \quad x = 0, \quad T = T_s \tag{7}$$

Solving Eqs. (1), (2) and (7), the solution for this case is:

$$\frac{T_s - T}{T_s - T_o} = \text{erf}\left(\frac{x}{2\sqrt{\alpha t}}\right) \tag{8}$$

Equation (8) can also be obtained by substituting $h = \infty$ and $T_a = T_s$ in Eq. (4).

3.1.3 Nonpenetrating Heat Flow

3.1.3.1 Constant Heat Flow

In this case, a constant heat flux (Q in $cal/cm^2 sec$) is absorbed by the upper surface of the skin, for example, from a hot radiator. The boundary condition becomes:

$$t > 0, \quad x = 0, \quad \partial T/\partial x = -Q/k \tag{9}$$

The solution of Eqs. (1), (2) and (9) is then:

$$T - T_o = \frac{Q}{k}\left\{2\sqrt{\frac{\alpha t}{\pi}}\, e^{-x^2/4\alpha t} - x\left[\text{erfc}\left(\frac{x}{2\sqrt{\alpha t}}\right)\right]\right\} \tag{10}$$

3.1.3.2 Square-Wave Pulse of Heat Flow

Equation (10) considers only the heating phase during thermal exposure. If the decrease of temperature after the heat source is removed, are taken into account. Equation (10) can be extended to include the cooling phase. For a square-wave pulse of heat source described as follows:

$0 < t \leq \tau, \quad Q = Q_1 = \text{constant}$

$t \leq 0 \quad \text{and} \quad t > \tau, \quad Q = 0$

where τ = exposure time, sec.

The equation suggested by Buettner (given in Weaver and Stoll [10]) is:

$$T - T_o = \frac{Q_1}{k}\left\{2\sqrt{\frac{\alpha t}{\pi}}\, e^{-x^2/4\alpha t} - x\left[\text{erfc}\left(\frac{x}{2\sqrt{\alpha t}}\right)\right]\right\}$$

$$- \frac{Q_1}{k}\left\{2\sqrt{\frac{\alpha(t-\tau)}{\pi}}\, e^{-x^2/4\alpha(t-\tau)} - x\left[\text{erfc}\left(\frac{x}{2\sqrt{\alpha(t-\tau)}}\right)\right]\right\} \tag{11}$$

Equation (11) is a two-part soluton. During the heating phase $0 < t \leq \tau$, the first term on the right hand side of Eq. (11) is real, while the second term is imaginary or zero. During the cooling phase $t > \tau$, both terms are real. As time approaches infinity, the first and second terms approach zero and thus T approaches T_o.

3.1.4 Penetrating Radiant Heat

Penetrating radiant heat refers to the radiation from the sun or an atomic bomb blast. Assuming the absorption of radiation in skin layers is analogous to many familiar types of radiation absorption such as that in CO_2 and H_2O, the decrease in intensity of the penetrating radiation transmitting through a layer is proportional to the thickness of the layer and the intensity of the radiation at that point [8]. Thus:

$$dI = - \nu I \, dx \tag{12}$$

Where I = penetrating heat flux, cal/cm^2sec

ν = absorption coefficient, cm^{-1}

Integrating Eq. (12) from the surface to a depth x gives:

$$I = I_s \, e^{-\nu x} \tag{13}$$

or

$$dI/dx = -I_s \nu \, e^{-\nu x} \tag{14}$$

where I_s = heat flux impinging at the surface. In this case, the energy balance equation of a skin element is no longer the same as Eq. (1). The new balance equation including the penetrating effect is:

$$\frac{\partial T}{\partial t} = \alpha \frac{\partial^2 T}{\partial x^2} + \frac{I_s \, \nu \, e^{-\nu x}}{\rho C} \tag{15}$$

Nevertheless, the initial condition remains unchanged (Eq. (2)), but the boundary condition becomes:

$$t > 0, \quad x = 0, \quad \frac{\partial T}{\partial x} = -\frac{R}{k} \tag{16}$$

where R = non-penetrating heat flux absorbed at the surface layer. Then, the solution for this case is

$$T - T_o = \frac{I_s e^{\nu^2 \alpha t}}{2 k \nu} \{ e^{-\nu x} \operatorname{erfc} (\nu \sqrt{\alpha t} - \frac{x}{2\sqrt{\alpha t}}) + e^{\nu x} \operatorname{erfc} (\nu \sqrt{\alpha t} + \frac{x}{2\sqrt{\alpha t}}) \} \tag{17}$$

$$- \frac{I_s e^{-\nu x}}{k \nu} + \frac{2(I_s + R)}{k} \sqrt{\frac{\alpha t}{\pi}} e^{-x^2/4\alpha t} - \frac{x(I_s + R)}{k} \operatorname{erfc} (\frac{x}{2\sqrt{\alpha t}})$$

Numerical results from the above equations are available in Refs. 5, 6 and 10. Typical time-temperature relationshps calculated from Equations (8), (10), (11) and (17) are given in Figures 3, 4, 5, and 6 respectively. As seen in Figure 6, when ν is greater than 100 cm^{-1}, the increase of surface temperature approaches to that for $\nu = \infty$. If $\nu = \infty$, Equation (17) reduces to Equation (10), the non-penetrating case.

Figure 3 Temperature Rises at Different Skin Layers Due to a Direct Contact Exposure. Figures on Curves indicate Time in Seconds. From Buettner [6]

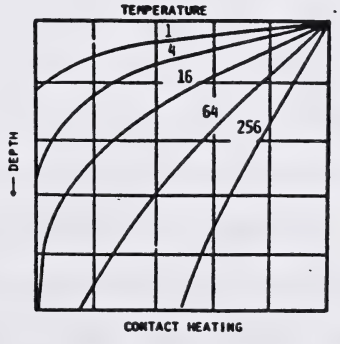

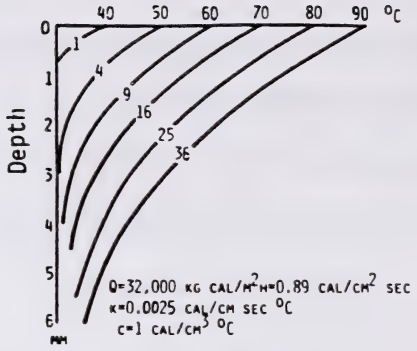

Figure 4 Temperature Rises at Different Skin Layers Due to a Non-penetrating Constant Heat Exposure. Figures on Curves Indicate Time in Seconds. From Buettner [6]

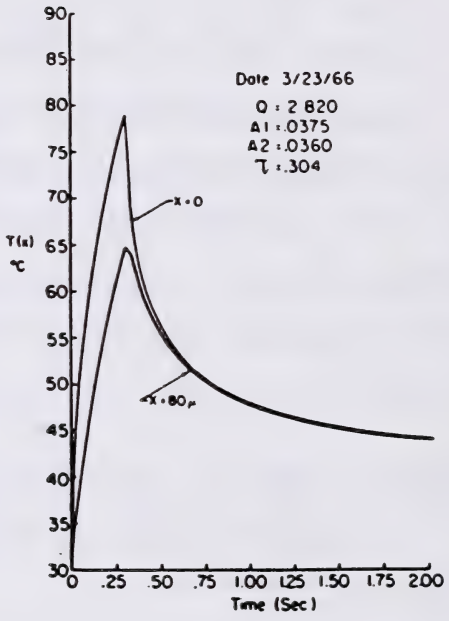

Figure 5 Temperature-Time History of Skin Exposed to a Square-Wave Pulse of Nonpenetrating Radiation. From Weaver and Stoll [10]

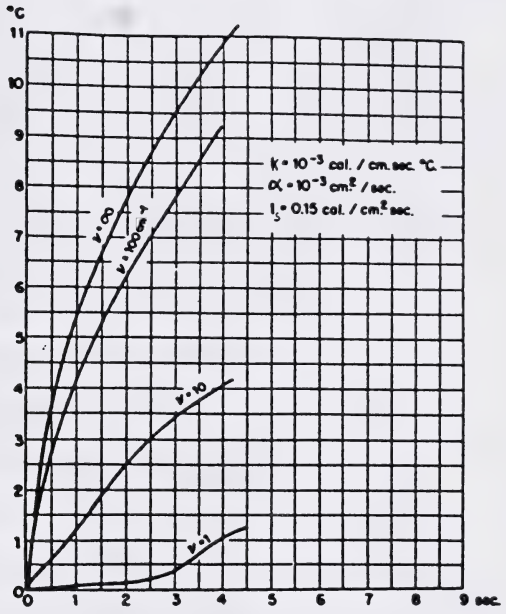

Figure 6 Increase of Skin Surface Temperature with Time During a Penetrating Radiation Exposure. From Buettner [6]

3.2 Analysis of Theoretical and Experimental Results

Henriques and Moritz [5] computed the temperature changes at the epidermal-dermal interface using Equations (4) and (8). They assumed that the epidermal thickness, x, was 80 μm and $x/(2\sqrt{\alpha}) = 0.15$ $\text{sec}^{1/2}$. The computed temperatures for the skin surface exposed to a hot environment and to a hot body by direct contact are shown in Tables 4 and 5 respectively.

Comparing the data in the tables, one finds that the temperature rise at the epidermal-dermal junction by means of convection and radiation (Table 4) is much slower than that by direct contact with a hot body (Table 5). In the latter case, the temperatures reach steady states after about 30 to 60 sec of exposure. Henriques and Moritz concluded that "for a given source temperature, a mechanism that enables the surface temperature to be immediately brought to, and maintained at, the source temperature has, on a

time basis, at least a thousand times greater propensity to injure the epidermis than a heat source which raises the skin temperature by means of radiation, and conduction and convection of relatively immobile air."

Table 4 The Computed Time-Temperature Relationships at the Basal Layer When an Entire Animal (~ 30 cm Diameter) Is Surrounded by an Envelope of Ambient Air and Radiant Heat with a Constant Temperature Source. From Henriques and Moritz [5]

	Circumambient temperature				
	80° C.	100° C.	125° C.	150° C.	175° C.
	Heat transfer coefficient, ° H, in calories per sq. cm. per minute per °C.				
	0.015	0.019	0.021	0.024	0.026
Time	Temperature at basal epidermal layer				
(seconds)					
0	35° C.	35° C.	35° C.	35° C.	35° C.
10	37	39	40.5	44	46
20				46.5	49
30	38.5	41.5	44	49	52
40				51	54.5
50	39.5	43.5	46.5	53	57
70	40	44	48	56	60
100	41	45.5	50	59	64
130	42	47	52	61	
160	42.5	48.5	54.5	63	
200	43	50	56	65	
300	45	52.5	59		
400	46	55	63		
500	47				
600	48				
800	50				
1000	50.5				
1200	51				

Table 5 The Computed Time-Temperature Relationships at the Basal Layer When the Skin Surface Is Immediately Brought to, and Maintained at, a Specific Temperature. From Henriques and Moritz [5]

	Surface temperature during heat exposure				
	45° C.	55° C.	65° C.	80° C.	100° C.
Time	Temperature at basal epidermal layer				
(seconds)					
0	35.0	35.0	35.0	35.0	35.0
0.01				36.3	37.0
0.02			38.9	40.9	43.4
0.05		41.8	45.2	50.3	57.1
0.1	40.1	45.2	50.3	57.9	68.2
0.2	41.3	47.6	53.9	63.3	75.9
0.5	42.7	50.4	58.1	69.6	85.1
1	43.3	51.6	60.0	72.4	89.1
2	43.8	52.6	61.4	74.6	92.3
5	44.2	53.5	62.7	76.6	95.1
10	44.5	53.9	63.4	77.6	96.6
30	44.7	54.4	64.1	78.6	98.0
60	44.8	54.6	64.4	79.0	98.6
120	44.9	54.9	64.5	79.4	99.2
300	44.9	54.9	64.7	79.5	99.3
600	44.9	54.9	64.8	79.7	99.6
Steady state	44.8	54.5	64.2		

Experiments were also carried out by Henriques and Moritz to study the change of dermis-fat interface temperature when the surface of porcine skin was immediately brought to, and maintained at, a constant temperature (Table 6). After 10 min. exposures to surface temperatures of 50 to 70°C, they found that the dermis (corium) thickness increased significantly due to the excessive accumulation of a clear yellowish fluid (edema) in the dermis. When the surface temperatures were maintained below 50°C, accumulation of edema fluid did not appear. Above 70°C, the dermis was denatured so that these mechanisms were destroyed. The presence of the edema fluid decreased the dermis temperature if the amount of edema fluid presented, more than compensated for the energy uptake. This effect was maximal when the skin surface was maintained at about 60°C.

Table 6 The Measured Time-Temperature Relationships for the Dermal-Fat Interface When the Skin Surface is Immediately Brought to, and Maintained at, a Specific Temperature. From Henriques and Moritz [5]

Initial	Skin surface temperature in °C. 35.0	34.8	34.8	35.2	34.9	34.3	34.2	34.5
During exposure	45	50	55	60	65	70	80	90
Time	Dermis-fat interface temperature in °C.							
(minutes)								
	34.7	34.5	34.6	35.0	34.7	34.2	34.4	34.8
0.2	36	38	39	43	46	52	53	56
0.5	38	43	45	46	52	62	65	66
1.0	39.5	45	47	48	53	65.6	71	74
1.5	40	47	48	47	53	66.5	72	77
2.0	40.5	47	49	46	54	67	74	79
3.0	41	47	48.5	45	56	67.5	75	79
5.0	42	47	47.5	44.5	58	67.5	77	
7.0	42	46.5	47.5	47	58			
10.0	42	47	48	49	59			
Initial	Average thickness of corium in mm. 2	2	2	2	2	2	2	2
At termination of exposure to heat	2	2.5	3.2	4.2	3	2.5	2	2
	In vivo thermal conductivity of dermis at termination of exposure 0.06	0.1	0.09	0.10	0.16			

Lipkin and Hardy [11] measured the surface temperature of human skin with and without blood flow obstructed by exposing the surface to a constant radiation of 0.055 cal/sec cm^2. Figure 7 shows the heating curves of the skin of the forearm. It is seen that the temperature of the normal skin increased to a maximum after about 60 sec of heating and then begin to drop. However, the temperature of the skin with blood flow obstructed kept increasing. Thus the influence of the blood flow which was increased in the normal skin due to heating causes a decrease in skin temperature in spite of continued irradiation. This phenomenon becomes apparent after the first 20 sec. of heating.

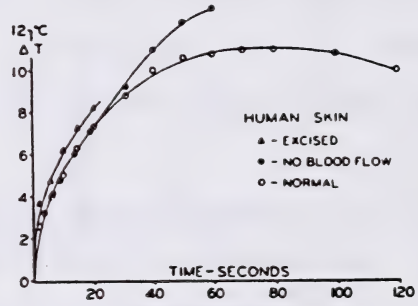

Figure 7 Surface Temperature of Human Forearm With and Without Blood Flow Obstruction When Exposed to a Radiation of 0.055 cal/cm^2 sec. From Lipkin and Hardy [11]

The effects of the presence of edema fluid and the change in blood flow cannot be observed in Tables 4 and 5. This is because constant thermal properties were assumed in the predictions. However, Henriques and Moritz mentioned that even neglecting the variations of the epidermal thermal conductivity and other factors results in uncertains of less than 0.2°C in the steady state temperature of the basal epidermal layer.

4. THE THERMAL PROPERTIES OF SKIN

The reaction of skin to heat application depends significantly on its thermal properties because these properties affect directly the change of skin temperature during heat transfer processes. The values of the properties such as conductivity (k), capacity (c), density (ρ), thermal inertia ($k\rho c$) and diffusivity ($\alpha = k/\rho c$) of cutaneous and subcutaneous tissues have been determined by several investigators. Some of these properties were found to vary considerably with layer, site, moisture content, irradiation and temperature. Excised skin also differs from living skin because of the increased blood flow due to heating.

Henriques and Moritz [5] estimated the heat capacity and thermal conductivity of dissected cutaneous and subcutaneous porcine tissues. They reported that the average conductivity for epidermis was 0.0005, dermis 0.0009, fat 0.0004 and muscle 0.0011 cal/cm sec°C. The average heat capacity for epidermis was 0.86, dermis 0.77, fat 0.55 and muscle 0.91 cal/g°C. The density of epidermis was assumed to be 0.8 g/cm^3. By exposing the skin surface of a pig to a predetermined temperature and maintaining this temperature at various levels between 45 and 90°C, they found that the thermal conductivity of dermis increased two to three-fold after 10 minute exposure due to the presence of edema fluid. On the other hand, evidence indicated that the thermal diffusivity ($\alpha = k/\rho c$) was probably not as sensitive as its individual quantities.

As reported in [5] and [11], the thermal conductivity of peripheral tissues of man, as determined by Lefevre, and the conductivity of fat and muscle for horse, pig, dog and cow, measured by Breuer are in good agreement with those obtained by Henriques and Moritz. However, the epidermal

density from Leider and Bunche (reported in [12]) is 1.1 to 1.2 g/cm^3, which is about 40 to 50% higher than that assumed by Henriques and Moritz. Their results with others are summarized in Table 7.

Shortly after Henriques and Moritz, Hensel (reported in [13]) used Eq. (8) in Section 3.1.2 to calculate the thermal diffusivity (α) for the layers from the surface down to the layers of interest by measuring the temperature wave propagating into the skin when contact heat was applied. About one year after Hensel, Buettner [13] used Eq. (10) to calculate the product of $k\rho c$ for surface heating of the various parts of human skin.

Table 7 Thermal Conductivity (k), Capacity (c) and Density (ρ) of Cutaneous and Subcutaneous Tissues

Thermal Properties	Epidermis	Dermis	Fat	Muscle	Remarks
k (cal/cm sec°C)	0.0005	0.00088	0.00038	0.00110	(1)
	0.0005	/	/	/	(2)
	/	/	0.00035	0.00100	(3)
	/	/	0.00049	0.00092	(4)
c (cal/g°C)	0.86	0.77	0.55	0.91	(1)
ρ (g/cm^3)	0.8	/	/	/	(1)
	1.1-1.2	/	/	/	(5)
	/	/	0.92	/	(6)
	/	/	/	1.27	(7)

(1) From Henriques and Moritz [5] for porcine tissues
(2) Lefevre's data for human tissues, reported in [11]
(3) Breuer's data for porcine tissues, reported in [5] and [11]
(4) Hatfield and Pugh's for human and beef fat, and human muscle, reported in [11]
(5) Leider and Bunche's reported in [12]
(6) Handbook of Chemistry and Physics, 1949
(7) From Lipkin and Hardy [11] for human muscle

At surface ($x = 0$, $T = T_s$), Eq. (10) becomes:

$$k\rho c = \frac{4\,Q^2\,t}{\pi(T_s - T_o)^2} \tag{18}$$

Thus, the product of $k\rho c$ can be evaluated if the temperature rise at the surface, the heat flux and the time are known. The radiation levels used in Buettner's evaluation ranged from 0.055 to 0.58 cal/cm^{2}sec. The average values of the products figured out by him were 0.0013, 0.0010 and 0.0023 cal^2/cm^{4}sec°C^2 for human forearm, body and finger tip, respectively. To calculate the conductivity from these products, Buettner assumed the ρc of the skin to be 0.8 cal/cm^3°C. He also calculated the conductivity for any intermediate layers based on Hensel's thermal diffusivity for the layers from the surface down to any layers concerned. The conductivity calculated by Buettner and the diffusivity determined by Hensel are shown in Table 8.

Table 8 Thermal Diffusivity ($k/\rho c$) and Conductivity (k) of Different Skin Layers, from Buettner [13]

Hensel's Data		Buettner's Data	
Layer (mm)	$k/\rho c$ (cm^2/sec)	Layer (mm)	k (cal/cm sec°C)
0 - 0.26	0.0004	0 - 0.26	0.0003
0 - 0.45	0.0006	0.26 - 0.45	0.0015
0 - 0.90	0.0010	0.45 - 0.90	0.0024
0 - 1.30	0.0013	0.90 - 1.30	0.0032

Lipkin and Hardy [11] entitled the $k\rho c$, the 'thermal inertia' for surface heating, because, according to Equation (18), the greater the $k\rho c$ the lesser the surface temperature rise will be for a given intensity of heat flux. Equation (18) was used again by Lipkin and Hardy to estimate the $k\rho c$. They studied dry and moist excised tissues, and living skin with blood flow intact and blood flow obstructed. In their studies, the levels

of radiation applied were around 0.04 to 0.06 $cal/cm^2 sec$. They found that loss of water in human muscle and excised skin appreciably decreased the 'thermal inertia', and increase of blood flow in intact skin decreased the rise of surface temperature, resulting in an increase in 'thermal inertia'. As shown in Table 9, the value of the 'inertia' for excised skin determined by them ranged from about 0.00055 for dry skin to 0.00075 $cal^2/cm^4 \cdot C^2$ sec for moist skin. However, the 'inertia' for living skin with blood flow obstructed was about 0.0009 $cal^2/cm^4 \cdot C^2 sec$. For living skin with blood flow intact, the 'inertia' varied from 0.0009 to 0.0040 $cal^2/cm^4 \cdot C^2 sec$ depending on the state of dilation of blood vessels. In order to set down a simple value of the inertia for surface heating for the living skin, Lipkin and Hardy suggested a value of 0.0009 to 0.0010 $cal^2/cm^4 \cdot C^2$ sec for short periods (20 sec or less) of heating by non-penetrating radiation of the dry skin of the face, hands, and forearms. While other work by Hardy, Goodell and Wolff (reported in [11]) indicated a slightly larger value of $k\rho c$ (0.00125 $cal^2/cm^4 \cdot C^2$ sec) for heating the forehead and hand within 3 sec. Further, Hardy and Oppel (reported in [11]) obtained a value of 0.00120 $cal^2/cm^4 \cdot C^2$ sec during the first 30 sec of heating of the face. Similarly, the thermal conductivity can also be calculated from these products. Lipkin and Hardy suggested a value of 1.20 g/cm^3 for the density and 0.81 cal/g°C for the thermal capacity.

Table 9 Thermal Inertia ($k\rho c$) of Human Tissues, from Lipkin and Hardy [11]

Tissues	$k\rho c$ ($cal^2/cm^4 sec°C^2$)
Muscle	0.00056 (dry) to 0.00113 (moist)
Fat	0.00026
Excised skin	0.00055 (dry) to 0.00075 (moist)
Living skin (blood flow obstruction)	0.0009
Living skin (blood flow intact)	0.0009 to 0.004 depending on state of vasodilatation

In addition to the dependence on layer, site, moisture content and blood flow rate, the thermal properties depend also on irradiation and tissue temperature. Stoll and Greene [12] repeated the method to find the change of thermal inertia of the skin with irradiance. Sites on the volar surface of the forearm were exposed to irradiances from 0.1 to 0.4 $cal/cm^2 sec$ until threshold pain was produced. The thermal inertia at pain threshold for different irradiances is given in Table 10. As shown, the average $k\rho c$ varied over a considerable range and increased with each increase in level of irradiance.

Table 10 Thermal Inertia ($k\rho c$) of Skin at Pain Threshold, from Stoll and Greene [12]

Irradiance ($cal/cm^2 sec$)	$k\rho c \times 10^{-5}$ ($cal^2/cm^4 sec°C^2$) Average	Range
0.10	96	75 - 117
0.15	110	89 - 142
0.20	127	95 - 158
0.30	139	115 - 168
0.40	159	144 - 181

Finally, Weaver and Stoll [10] studied the variations of the thermal conductivity with tissue temperature for both heating and cooling phases using Eq. (11). They assumed that $\rho c \approx 1$ cal/cm^3°C for human skin so that $\alpha \approx k$ and the conductivity remains constant from the surface inward to the basal layer, the interface between the dermis and the epidermis. Thus, Eq. (11) can be solved for either the thermal diffusivity or the conductivity for any given experimental time-temperature history at 80 μm, the best value for the depth of the basal layer in the volar surface of the forearm ([5, 10]). Some of their results are given in Fig. 8 in which each of the curves can be separated into two curves. The upper curve sloping downward to the right represents a continuous heating to a peak temperature of about 52 to 57°C depending on the radiation levels. The lower curve sloping downward to the left represents a continuous cooling from the peak temperature back to 44°C. The exposure time for each curve is the shortest time required to produce blistering within 24 hours (blistering may be delayed in some instances, see Section 5.1), and ranges from 5.56 to 33.80 sec depending on the radiation. As seen in the figure, the thermal conductivity decreases continuously when the tissue temperature increases during the heating phase. During the cooling phase, the conductivity decreases with the tissue temperature. The greatest variations occur at temperatures below 44°C, but little variation occurs at temperatures above 44°C. The effects of the presence of edema fluid and the increase of blood flow due to continuous heating were not mentioned in their paper.

Another thermal property that has not yet been discussed is the absorption coefficient (ν). This coefficient is significant only when penetrating radiation is considered. Buettner ([6], [13]) found that the

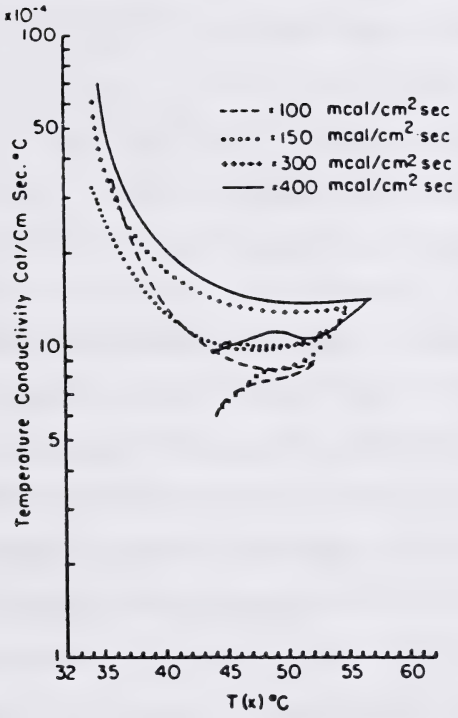

Figure 8 Variations of the Thermal Conductivity of Human Skin with Tissue Temperature at 80 μm deep. From Weaver and Stoll [10]

absorption coefficient of human skin was between 100 and 1000 cm^{-1} for the spectrum of infrared radiation. Since this coefficient is very large, infrared radiation does not penetrate the skin. The solar rays, however, showed a ν near 10 cm^{-1}. According to Refs. 6 and 14, the spectrum of the radiation from an atomic bomb blast may be considered close to that of the sun. Thus a value ν = 10 cm^{-1} can be assumed for this case.

5. THE QUANTITATIVE, QUALITATIVE AND SENSATIONAL EFFECTS OF HEAT ON THE SKIN

Reactions of skin to heat applications, ultimately result in cutaneous burns. The severity of burns may be characterized quantitatively according to the depth to which the tissue has been destroyed, or qualitatively according to the nature of the changes that have occurred, or even sensationally according to the intensity of pain induced.

5.1 General Consideration of the Quantitative and Qualitative Effects

Moritz [15] studied both the quantitative and qualitative effects of heat on the skin. He indicated that the mildest form of epidermal injury produced by burning was latent in the sense that alteration in cell structure were unable to be recognized, although temporary impairment in the adhesion between epidermis and dermis were observed. Such injuries were reversible and the time required for their recovery increased with the time required for their production.

The first evidence of irreversible thermal injury of the epidermis was a redistribution of water and solids within the nuclei of the epidermal cells. As a result, the nuclei swelled, first in the intermediate and later in the deepest layer. Further injury resulted in swelling and disintegration of the cytoplasm (a complex, jelly-like colloidal substance constituting the living matter outside a cell nucleus) of the basal cells and pyknosis (thickening and shrinking through degeneration) of nuclei throughout the entire thickness of the epidermis. When the temperature within the epidermis was less than about 55°C, further primary thermal alterations of the epidermal cells were negligible. When the temperature exceeds approximately 55°C, coagulation occurred. Coagulative changes

might mask both nuclear swelling and cytoplasmic disintegration. Further increases in temperature resulted in desiccation and eventually in carbonization.

The earliest visible alternative change in the dermis was constriction of the superficial blood vessels. Normally, this was followed immediately by dilation. Thermal dilation of superficial blood vessels lead to increased vascular permeability and edema formation. When a heat exposure was sufficient to damage the attachment between epidermis and dermis, the amount of edema fluid that collected between them was usually sufficient to elevate and to form a blister. Therefore, blistering customarily indicated destruction of epidermis. However, absence of blisters did not always indicate epidermal survival because there were several instances in which blistering was either delayed or prevented.

Delayed blistering was most often observed after long exposures at low temperatures or after flash exposures at high temperatures. In both cases, the exposures were either too low in intensity or too short in duration to cause sufficient vascular damage. As a result, long hours (usually within 24 hours) were required to collect enough fluid under the damaged epidermis to form a blister. Also, after extreme exposures, the dermis and its superficial blood vessels were almost immediately coagulated. In this case, blood flow through superficial capillaries was stopped and edema developed was too deep to produce blistering.

Like the epidermis, coagulative changes occurred in the dermis at a temperature of approximately 55°C or above. Further increases in dermal temperature might result in desiccation and carbonization. Thus, for a exposure of insufficient intensity to raise the epidermal or dermal

temperature above 55°C, coagulation did not occur even though deep destruction might be produced if sufficiently prolonged. while a relatively shallow burn might show coagulation and even carbonization if the exposure had been intense and short.

The depth to which the tissue was destroyed (the quantitative reaction), on the other hand, increased with both the duration and intensity of exposures. But the duration and intensity of exposures to produce similar quantitative reactions were inversely related. In this case, the quantitative results of a short exposure of high intensity may be similar to those of a long exposure at low intensity. As discussed previously, a high intensity exposure usually results in a coagulative type of burn and a low intensity results in a non-coagulative type of burn. Apparently, quantitative similarity between reactions does not necessarily mean that the reactions are qualitatively similar. Therefore, the superficial appearance of a burn is not a reliable criterion for judging the depth to which the tissue may have been destroyed [15].

In order to classify the severity of thermal injury quantitatively, cutaneous burns, according to [15, 16] were characterized as first, second, or third degree. First degree burns referred to the cutaneous reactions that indicated incomplete destruction of the epidermis. Second degree burns were defined as the reactions that indicated complete destruction of the epidermis without a significant degree of injury to the dermis. Reactions indicative of a complete destruction of the epidermis and a serious damage to the dermis were designated as third degree.

5.2 General Consideration of the Sensational Effect

Pain is the primary sensational effect of heat on skin. The intensity of pain caused by cutaneous burning can be explained according to the concept introduced by Weber (reported in [17]). The Weber Law states that as the intensity of a stimulus increases, the ability to discriminate differences in intensity of stimulus decreases proportionately. In other words, as the intensity (I) of a stimulus increases, the minimum change in intensity (ΔI_m), which can just barely be distinguished or felt when added to or subtracted from I, increases proportionately. That is:

$$\frac{\Delta I_m}{I} = C_1 \tag{19}$$

in which $\Delta I_m/I$ is known as the Weber ratio and C_1 is a constant.

Fechner extended Equation (19) to relate the sensation to the stimulation by assuming that for a given intensity of stimulus (I), the factor by which the change in intensity of stimulus (ΔI) exceeds the "just noticeable difference" in intensity (ΔI_m) is proportional to the change in sensation (ΔS). That is:

$$\frac{\Delta I}{\Delta I_m} = C_2 \Delta S \tag{20}$$

Substituting Equation (20) into Equation (19) gives:

$$\frac{\Delta I}{I} = k \Delta S \tag{21}$$

where $k = C_1 C_2$. Upon integration from the threshold stimulus intensity I_o to an intensity I, the corresponding intensity of sensation S is:

$$S = S_o + k \log I/I_o \tag{22}$$

where S_o = threshold sensation.

Thus, Equation (22) can be used to evaluate the intensity of pain sensation for any types of thermal stimulus.

A scale of pain intensity has been established by Hardy, Wolff and Goodell [17]. They measured the "just noticeable difference" in intensity of thermal radiation stimulus (ΔI_m) for each increase in radiation level starting at the intensity at which threshold pain occurred to the intensity at which further increase in radiation caused no perceptibly greater pain. The pain induced by this maximal magnitude of radiation is therefore a "ceiling" pain. They found that there were 21 discriminate intensities of pain between the pain threshold and the ceiling pain. Hardy et al., then, set up a pain intensity scale in terms of just noticeable difference (JND) according to the assumption of Fechner that the intensity of sensation evoked by a given stimulus was equivalent to the number of the discriminable steps from the threshold sensation. Thus, a value of 0 JND indicates the beginning of the scale or no pain and a value of 21 JND indicates the maximum of pain intensity. Another unit of pain intensity called "dol" was also proposed by them. They defined 1 dol = 2 JND. Figure 9 indicates the pain intensity, in terms of both dol and JND, induced by heating the forehead and forearm for a duration of 3 sec. As shown, a pain threshold was produced at about 0.22 cal/cm^{2}sec for a 3 sec exposure. When the intensity was increased above 0.48 cal/cm^{2}sec, it was not until the stimulus had been increased to 0.68 cal/cm^{2}sec that a barely perceptible difference from 0.48 cal/cm^{2}sec could be noted. Although intensity beyond 0.68 cal/cm^{2}sec could be distinguished from 0.48 cal/cm^{2}sec, it was not possible to distinguish any stimuli greater than 0.68 from 0.68 cal/cm^{2}sec. Therefore, the sensation evoked by a stimulus

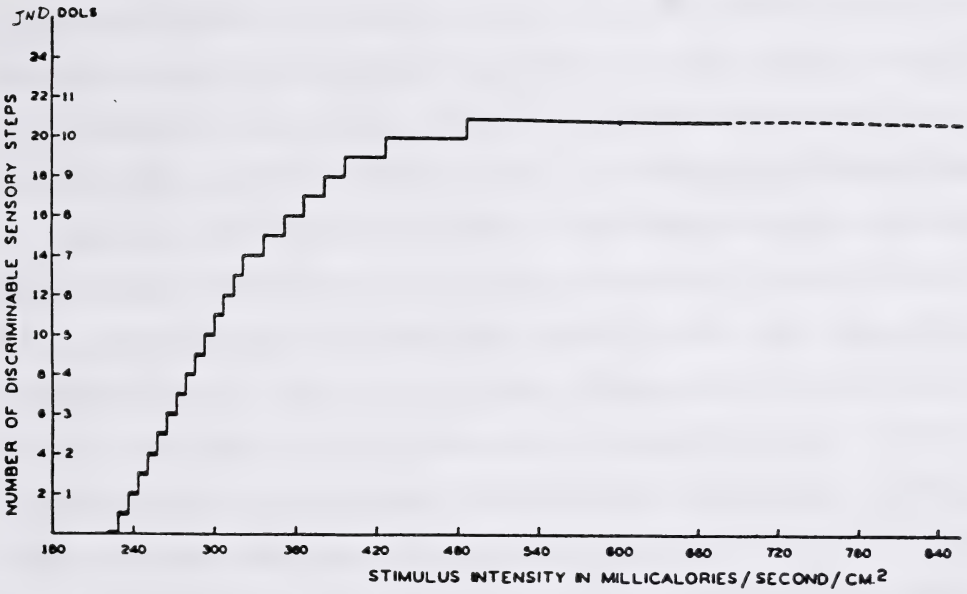

Figure 9 Pain Intensity Induced by Heating the Forehead and Forearm for a Duration of 3 Seconds. From Hardy, Wolff and Goodell [17]

of about 0.68 cal/cm^{2}sec was the ceiling pain and no greater pain could be felt beyond this point. Hardy et al. also indicated that beginning at the threshold the type of cutaneous pain was a pricking sensation and after the stimulus intensity was increased to about 0.32 cal/cm^{2}sec, a burning quality of pain was added to the total sensation.

5.3 Thresholds of Burns, Blistering and Pain as Related to the Intensity and Duration of Thermal Exposure

The time-temperature thresholds for first and second degree burns in pigs and men have been studied by Moritz and Henriques [16] (pigs were used because porcine skin is similar to human skin). Although it was found that a pig did not sweat like a man, and that there were certain qualitative differences in the responses of human and porcine skin to heat application,

there were no significant quantitative differences in their sensitiveness to thermal injury. Moritz and Henriques also discovered that porcine skin was not uniformly sensitive to thermal injury. The skin of the neck and the mid-portion of the back was found to be less sensitive than that of the lateral portion of the shoulders, thorax and abdomen. While the most sensitive areas were the portions on the ears, thighs, buttocks and ventral surface. For human skins, Buettner [13] illustrated that the forearm appeared to be less susceptible to thermal injury than any other parts of the body (e.g. forehead, chest, upper arm, palm, leg, etc.).

Moritz and Henriques obtained the overall results of the time-temperature thresholds at which cutaneous burns occurred, resulting from 179 exposures of porcine skin and 33 exposures of human skin on different parts of the body. Their results are plotted in Figure 10 in which the surface temperature was attained by contacting the skin surface directly with a rapidly flowing stream of hot water or oil maintained at constant temperatures. The crosses fitted by the solid line represent the minimum exposures that caused complete destruction of porcine epidermis (second degree threshold). Any exposures situated above the solid line are supra-threshold and those situated below are sub-threshold. The broken line represents the maximum exposures that failed to destroy porcine epidermis (first degree threshold). Thus exposures lying below the broken line cause no appreciable injury. Reactions of human skin are indicated by the circles. The solid circles indicate the second degree threshold. while the open circles represent the first degree threshold. As seen, there are no significant differences in the time-temperature thresholds between human and porcine skins.

Figure 10 indicates an inverse relationship between the surface temperature and the time required to produce first or second degree burns. The minimum surface temperature required to produce a threshold burn is about 44°C and the time is about 6 hours. At surface temperatures between 44°C and 51°C, the rate at which burning occurs increases logarithmically with a linear increase in skin temperature. Moritz and Henriques mentioned that in the case of surface temperature under 51°C the total exposure time required to destroy the epidermis was (a) so long that the time required to bring the temperature at the basal layer to a steady state was comparatively negligible, and (b) essentially equal to the total duration of the steady thermal state within the epidermis.

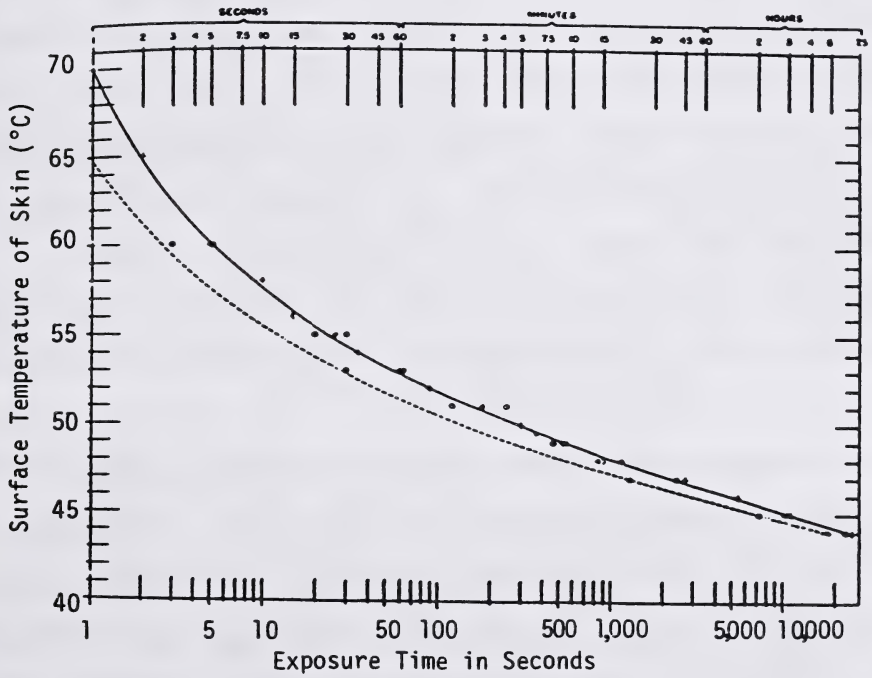

Figure 10 **Time-Surface Temperature Thresholds at Which Cutaneous Burning Occurs. From Moritz and Henriques [16].**

At surface temperatures above 51°C, the rate of injury increases rapidly and the pre-burn time is too short to allow the epidermis to reach steady state. Consequently, the relationship between the surface temperature and the pre-burn time is no longer linear. Above 70°C, a second degree burn can be produced in less than 1 second.

The same type of temperature-time threshold curve as presented by Moritz and Henriques has been confirmed by other investigators. They found that all these data could be represented by a simple exponential function [18]:

$$t = t_{ref} e^{(T_{ref} - T)} \tag{23}$$

where t_{ref} and T_{ref} are the reference time and temperature respectively.

Similarly, the thresholds of pain and blistering produced by exposures of thermal radiation have also be determined [12, 19, 20]. Figure 11 illustrates the tolerance times for different levels of thermal energy which are plotted on log log coordinates [20]. In this figure, the tolerance time represents the time required to produce threshold pain and minimal blistering (i.e. several small blisters appearing within 24 hours). These results were obtained from exposures of the volar surface of human forearm with an initial skin temperature of 32.5°C. As seen, a similar inverse relationship between the tolerance time and the intensity of absorbed energy appears in both the threshold curves of pain and blistering. The area between the 2 curves represents the region of suprathreshold pain and reversible tissue damage. The area above the blister curve represents the region of irreversible injury and below the pain curve, the safety zone. The survival curve in between the pain and blister curves is of no interest at the present time and, so, will not be discussed.

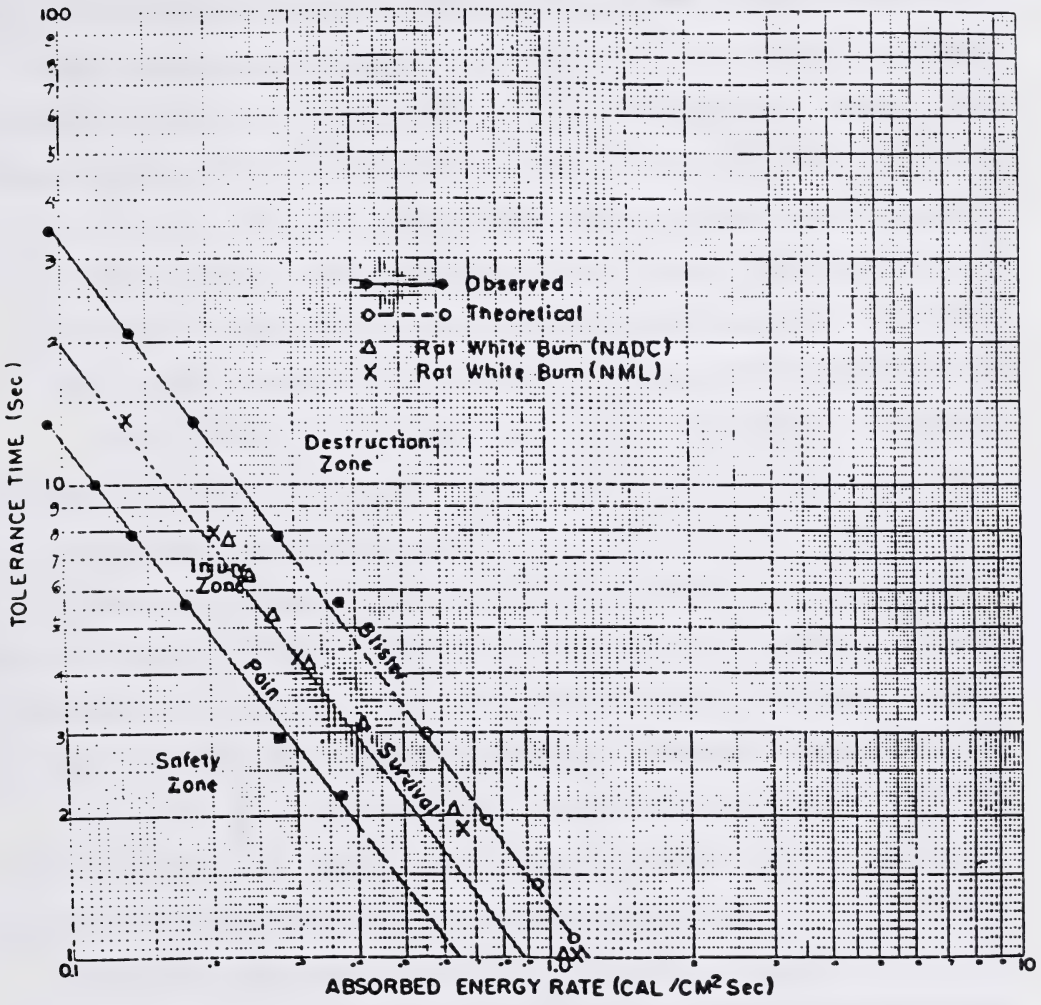

Figure 11 Human Skin Tolerance Time to Absorbed Thermal Energy. From Stoll and Chianta [20]

As shown in Figure 11, the intensity and duration at which threshold blistering occurs range from 0.1 cal/cm^2 sec in about 33 sec to 1.3 cal/cm^2 sec in less than 1 sec. For the pain threshold, the range is between 0.1 cal/cm^2 sec in approximately 13 sec and 0.64 cal/cm^2 sec in about 1 sec.

Although threshold pain and blistering are functions of both exposure time and radiation level, threshold pain occurs at some definite temperature, almost independently of the time required to attain this temperature, and also independently of the site of the body, whereas blistering depends strongly on both temperature and time [12, 13, 19].

As reported by Hardy, Jacobs and Meixner [19], threshold pain was elicited at a surface temperature of about 45.7°C (Table 11) and ceiling pain at about 60°C (Figure 12) regardless of the time of exposure and intensity of stimulus. In this case, the intensity of pain can be expressed simply in terms of the surface temperature as shown in Figure 12.

However, Stoll and Greene [12] illustrated that the skin surface temperature at pain threshold, instead of being a constant as shown in Table 11, tended to slightly increase at higher radiation levels due to the greater temperature gradient within the dermis at the higher intensities, but the threshold temperature of the pain receptors at an average depth of about 0.2 mm was invariable (about 43.2°C) throughout the range of irradiances between 0.1 and 0.4 cal/cm^2 sec. Since the 0.2 mm depth was calculated on the basis of the data obtained from exposures of the forearm, Stoll and Greene pointed out that (a) this value was much too thick for epidermis on the forearm, the effective pain receptors were therefore located in the dermis, and (b) the significance of this location was that it was theoretically feasible to destroy completely the epidermis without causing any pain, as long as the temperature gradient through the skin was such that the epidermal temperature was maintained at a threshold or suprathreshold level while the pain receptors were maintained at a sub-

Table 11 Stimulus Intensity, Exposure Time and Skin Surface Temperature at Pain Threshold. From Hardy, Jacobs and Meixner [19]

Exposure Time	Average Threshold Stimulus Intensity	Average Skin Temperature, °C at the surface	
		Initial	Threshold, calculated
sec.	mcal/sec/cm²		
0.25	708	34.0	45.3
0.57	424	34.4	44.3
1.02	347	34.3	45.5
1.24	304	34.9	45.6
1.50	293	34.3	45.7
1.96	263	34.3	45.9
2.40	241	34.1	46.0
3.20	199	34.4	45.9
4.11	175	34.6	45.8
4.83	154	34.5	45.2
8.00	130	34.2	46.1
10.00	108	34.8	45.8
22.00	66	35.3	45.5
45.00	52	35.1	46.5
60.00	47	34.2	46.0
300.00	39	34.2	No pain
Av. 45.7 S. D. ±1.7			

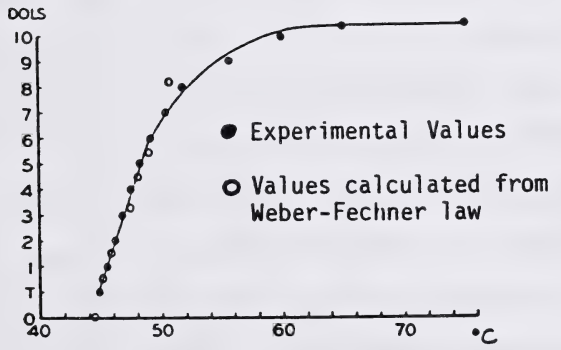

Figure 12 Relationship Between Pain Intensity and Skin Surface Temperature Obtained by Heating the Surface of the Forehead. From Hardy, Jacobs and Meixner [19].

threshold level. This is probably the reason why, as mentioned in [19], thermal injury without pain and pain without apparent injury are common experiences.

Before Stoll and Greene, Buettner [13] indicated that 'unbearable' pain, i.e. not the least perceptible pain as discussed previously, occurred at a threshold temperature of about 44.8°C at a depth of 0.1 mm rather than 0.2 mm. While other investigators argued that free nerve endings in the epidermis might mediate pain [12].

5.4 Factors Affecting the Effects of Thermal Exposure on the Skin

The possiblity of altering the vulnerability of skin to thermal injury by changing the initial skin temperature, blood pressure and water content of the skin has also been studied. It was found that a change in initial skin temperature did not alter the pain threshold temperature but the times required to produce threshold pain and burns were significantly affected during radiation exposures [12, 13, 19]. Stoll and Greene [12] demonstrated that the rate at which burning occurred were markedly increased even though the initial temperature was increased by only 1°C for the same intensity of irradiance. The initial skin temperature measured by them was 32.5°C. Buettner [13] indicated that precooling the skin from an average initial temperature of about 33°C significantly delayed the production of pain and burns. In the case of direct thermal contact, Henriques [21] mentioned that the effect of initial temperature on the rate of change of basal layer temperature was relatively insignificant. He suggested a value of 35°C for the initial skin temperature.

Changes in blood pressure by compression of the skin, on the other hand, showed little effect on the susceptibility to thermal injury although it altered the surface color of the burns [15, 16]. Alteration of water content by wetting the skin, according to [13], exerted no appreciably influence on the threshold time-intensity relationships at intensities of radiation above 0.25 cal/cm^2 sec. At about 0.055 cal/cm^2 sec, wet skin was found to be less sensitive than dry skin nevertheless the threshold pain temperature remained unchanged.

Another factor which is worthy of mention is the cumulative effects of repeated subthreshold exposures. Although a single subthreshold exposure causes no recognizable epidermal injury, latent injury may be sustained. When several subthreshold exposures are repeatedly applied to the same area, latent injury produced by each exposure can be accumulated to become recognizable injury if the intervals between exposures are shorter than the time required for their recovery.

Table 12 demonstrates this effect on the porcine skin. Exposures were made with a running stream of hot water at 49°C and at atmospheric pressure [16]. Exposures identified by Reference Nos. 1 to 18 are single exposures for control purposes. As seen, single exposures for less than 7 minutes cause no recognizable epidermal injury. Repeated exposures are indicated by Nos. 19 to 39. Though a single 3 minute exposure causes no recognizable injury, three such exposures each separated by recovery periods less than 48 minutes have the same effect as a single continuous 9 minute exposure. For intervals between exposures greater than 48 minutes, appreciable recovery was observed. Complete recovery requires 2 to 4 hours as indicated by Experiments 30 and 31.

Table 12 The Cumulative Effects of Repeated Subthreshold Thermal Exposures* on Porcine Skin. From Moritz and Henriques [16]

Duration of each exposure	No. of exposures at same site	Interval between exposures	Effect of exposure on skin				Reference no.
			No evidence of epidermal injury		Epidermal necrosis**		
			Mild vascular reaction	Severe vascular reaction	Focal	Complete and irreversible	
(minutes)							
3	1		x				1
3	1		x				2
3	1		x				3
4	1		x				4
5	1		x				5
6	1			x			6
6	1			x			7
6	1			x			8
7	1			x			9
7	1				x		10
8	1				x		11
8	1				x		12
8	1					x	13
9	1					x	14
9	1					x	15
9	1					x	16
9	1					x	17
9	1					x	18
3	3	3 min.				x	19
3	3	3 min.				x	20
3	3	3 min.				x	21
3	3	6 min.				x	22
3	3	12 min.				x	23
3	3	24 min.				x	24
3	3	48 min.				x	25
3	3	48 min.			x		26
3	3	72 min.			x		27
3	3	72 min.			x		28
3	3	96 min.			x		29
3	3	120 min.		x			30
3	3	240 min.	x				31
3	3	24 hrs.	x				32
3	3	48 hrs.	x				33
2	5	2 min.				x	34
2	5	30 min.	x				35
2	5	60 min.	x				36
3	2	12 min.		x			37
5	2	60 min.				x	38
5	2	240 min.			x		39

*All exposures were made to water at 49°C

**The sum of the morphological changes indicative of cell death and caused by the progressive degradative action of enzymes

Comparing the exposures from Nos. 34 to 39, one finds that the time required for recovery from latent injury, as would be expected, increased with the time of exposure. Therefore, the degree of recovery depends partly on the length of the recovery period and partly on the duration of exposure which causes unrecognizable injury.

6. PREDICTION OF CUMULATIVE TISSUE DAMAGE INCURRED DURING A BURN AND ITS RELATION TO PAIN INTENSITY

Before predicting the tissue damage and its relation to pain intensity, it is necessary to understand briefly the physical and chemical processes that take part in cell death during a burn. These processes, according to Henriques [21], can be basically classified into three general groups:

(a) Thermal denaturation of proteins - Living cells are primarily protein in nature. These proteins which participate in the maintenance of normal cell life are very sensitive to heat.

(b) Other changes in metabolic processes regardless of their effect on protein - For instance, increase in tissue temperature may alter the rate of diffusion, formation and degradation of chemical reactants. This will lead to a change in the concentrations of some of the individual constituents. Consequently, the entire metabolic equilibrium may be disturbed.

(c) Alterations in the physical characteristics of cells - This group includes all physical phenomena that are characteristic of protoplasm (a complex, jellylike celloidal substance constituting the living matter of a cell) but are not essentially affected by the thermal degradation of proteins, for example, diffusion through liquids and membranes, changes in viscosity, rigidity and liquefaction. All these biophysical processes are potentially able to cause cell death.

For any of the above processes to take place, the constituents involved should possess an energy content which is sufficiently high to activate the process. The minimum amount of energy required for the process to proceed is known as the activation energy. The rate of the process depends directly on the fraction of the constituents which have an energy content at least equal to the activation energy. In most chemical and physical processes, this fraction (f) based on the Maxwell-Boltzman energy distribution law [22] is:

$$f = e^{-\Delta E/RT} \tag{24}$$

where ΔE = activation energy, cal/mole

R = gas constant $\simeq$ 2 cal/mol K

T = temperature in K

Henriques assumed that the rate of any conceivable process that might result in cell death could be expressed in a formula similar to that for most chemical rate processes, the Arrhenius equation [22]. Thus:

$$\frac{d\Omega}{dt} = P\, e^{-\Delta E/RT} \tag{25}$$

where $d\Omega/dt$ = rate of cell damage, sec^{-1}

Ω = an arbitrary function to represent the amount of cell damage

T = tissue temperature in K

P = constant, sec^{-1}

Then the cumulative damage is:

$$\Omega = P \int_o^t e^{-\Delta E/RT}\, dt \tag{26}$$

As described in Section 5.3, when the skin surface is maintained at a temperature less than 50°C during exposures by direct thermal contact, the total exposure time required to reach second degree burn threshold is essentially equal to the total duration of the steady thermal state within the epidermis. In this case, the temperature at the basal layer can be considered invariant and equal to the steady state temperature. Equation (26) can be integrated to obtain:

$$\Omega = P\, t\, e^{-\Delta E/RT} \tag{27}$$

or

$$\ln t = \ln \Omega - \ln P + \Delta E/RT \tag{28}$$

Henriques assigned $\Omega = 1$ to represent the second degree burn threshold (damage just sufficient to cause complete destruction of the epidermis). Together with the data given in Figure 10 for surface temperatures less than 50°C, the constant P and the overall activation energy ΔE including

all the processes involved in cell damage can be obtained from the intercept and slope of the plot ln t vs. 1/RT (Equation (28)). These values were found to be:

$$P = 3.1 \times 10^{98} \text{ sec}^{-1} \quad (29)$$

$$\Delta E = 150{,}000 \text{ cal/mole} \quad (30)$$

Substituting Equations (29) and (30), and the data pertaining to the first degree burn threshold in Figure 10 back to Equation (28), the best fitted damage function representing the maximum damage condition before occurrence of irreversible epidermal injury is:

$$\Omega = 0.53 \quad (31)$$

Although the values of P, ΔE, and Ω were obtained by using Equation (27) and a limited portion of the experimental data, Henriques found that Equation (26), with these values of P and ΔE provided, could accurately predict the degree of epidermal injury in terms of the above defined Ω over the entire experimental temperature range for both direct contact and ambient hot air exposures, as long as the temperature history at the basal layer was known.

Henriques also found that of all of the physical and chemical processes potentially capable of causing cell damage, only the process of protein denaturation had an activation energy roughly equal to 150,000 cal/mole. The other processes had far lower activation energy. In this case, Henriques concluded that thermally induced epidermal injury was mainly the result of thermal alterations of those cellular proteins whose rate of denaturation corresponded to an activation energy of at least 150,000 cal/mole.

Stoll and Greene [12] used the rate process model as derived by Henriques to estimate skin damage due to thermal radiation. They measured the temperature history at the skin surface for each irradiance used. Based on these temperatures, the tissue temperature at a depth of 80 μm, approximately the basal layer, at every instant in time was calculated using Equation (8) in Section 3.1.2. Although Equation (8) is not for thermal radiation exposure, Stoll and Greene claimed that this equation was equally valid when the surface temperature at every instant was known. The calculated tissue temperature was then substituted into Equation (25) to solve for the rate of damage $d\Omega/dt$. By plotting $d\Omega/dt$ against the time at which the tissue temperature occurred, the area under the resultant curve was then the cumulative damage of the epidermis. For the production of threshold blistering which is equivalent to the second degree burn threshold, Stoll and Greene found that the total damage, including the damage done during both heating and cooling phases, was about two-tenths of the value obtained by Henriques for the same injury.

Upon analysis of all the possible reasons for this discrepancy, Stoll and Greene commented that since the steady state was never achieved at skin temperatures above 50°C in conductive heating, there might be a discontinuity in the damage rate function which was inconspicuous by the transition from the steady state to the unsteady state conditions. They further commented that the damage imposed after the exposure was removed should not be overlooked, especially at high intensity. As they mentioned, about 35% of the total damage was incurred during the return of the tissue temperature to the initial level at intensity of 0.4 cal/cm^2 sec (about 10% at 0.1 cal/cm^2 sec). In order to fit all their data to the rate process model to

yield $\Omega = 1$ to represent the total damage performed during heating and cooling at the blister threshold, they obtained the curve shown in Figure 13, which indicates the log of the damage rate against the tissue temperature at 80 μm. The damage rate at tissue temperature for conductive heating from Henriques is also presented.

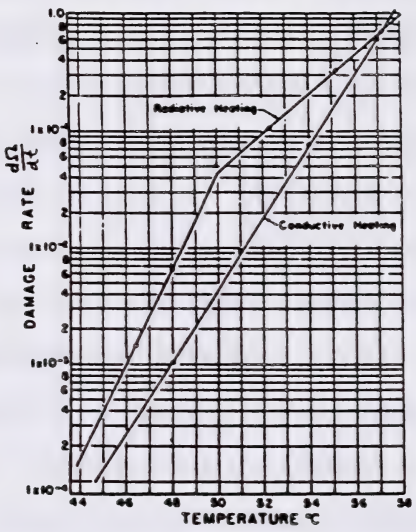

Figure 13 The Damage Rate Against the Tissue Temperature at 80 μm Such That $\Omega = 1$ at Threshold Blistering. From Stoll and Greene [12].

To relate pain to tissue damage, Hardy et al. [19] analyzed the basic event underlying 'noxious stimulation' resulting from thermal impact ('noxious stimulation' refers to the effect evoked at the pain fiber endings, i.e. pain, reflex response, etc., rather than to the type of stimulation used to produce these responses). They discovered that tissue damage, protein denaturation, pain and reflex responses (e.g. withdrawal of exposed area in man; contraction of muscle in guinea pig; and tail flick in

rat in response to thermal stimulus) all began at a threshold temperature of about 45°C. This temperature held in spite of the type, intensity and duration of thermal stimulus and also regardless of the initial skin temperature. Hardy et al. inferred that the same process underlined noxious stimulation and tissue damage, that is thermal denaturation of cellular proteins. Although thermally induced pain and damage can be explained as the results of the same process, pain depends only on the temperature to which the skin is raised while tissue damage depends on both temperature and time. From this standpoint, Hardy et al. further inferred that noxious stimulation of the skin eliciting pain was dependent on the rate of damage ($d\Omega/dt$) rather than the amount of damage (Ω) induced during a burn. This is because Equation (25) is a function of temperature only, whereas Equation (26) is a function of time and temperature. Based on this assumption, the stimulus (I) in Equation (22) for pain (S) can be represented by the damage rate ($d\Omega/dt$). Thus the relationship between pain and tissue damage can be expressed according to the Weber-Fechner law (Equation (22)) as:

$$S = S_o + k \log \dot{\Omega}/\dot{\Omega}_o \qquad (32)$$

where S = pain intensity
S_o = threshold pain
k = constant
$\dot{\Omega}$ = $d\Omega/dt$ = damage rate
$\dot{\Omega}_o$ = damage rate at pain threshold

As a first attempt, Hardy et al. combined Equations (32) and (25) to calculate the pain intensity and its corresponding skin surface temperature using the rate model developed by Henriques. The calculated values were then compared with the experimental values. They failed at pain

intensities above 17 JND (8.5 dol, see Figure 12). Later, Stoll and Greene repeated the procedures to find the relationship between tissue temperature at 80 μm, damage rate and pain intensity. This time, they used their own damage rate data (Figure 13) instead of the data from Henriques. They successfully obtained the correlation shown in Figure 14. It should be noted that the JND and temperature in the abscissa of Figure 14 are not corresponding to each other. The abscissa actually represents two axes overlapping each other. That is, the two curves in the figure are the projections of a single curve in space. This relationship is also tabulated in Table 13. Since it has been shown that threshold blistering occurs within 24 hours when $\Omega = 1$, and, the damage rate corresponding to a constant tissue temperature or pain intensity remains constant, then the time to blistering at a constant tissue temperature or pain intensity can be predicted by the reciprocal of the damage rate at which the temperature or pain intensity is maintained (Table 13).

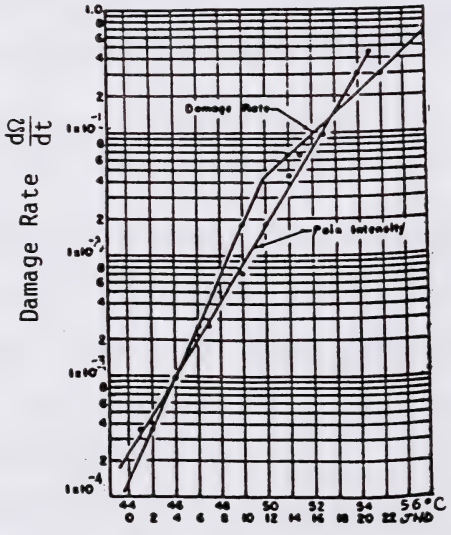

Figure 14 Correlation of Pain Intensity with Damage Rate and Tissue Temperature at 80 μm. From Stoll and Greene [12]

Table 13 Relationship Between Pain, Tissue Temperature and Damage Rate. From Stoll and Greene [12]

Observed Pain Intensity (JND)	Tissue Temperature at 80 μm (°C)	Damage Rate $\dot{\Omega}$ (sec^{-1})	$\dot{\Omega}/\dot{\Omega}_o$	Predicted Time to Threshold Blister when Ω=1 (sec)
1	45	0.00033	1.0	3300.0
2		0.00047	1.4	2130.0
4	46	0.00097	2.9	1030.0
8		0.00420	12.4	228.0
10	48	0.00840	25.4	118.0
12		0.01800	54.5	56.0
14	50	0.03600	109.0	28.0
16		0.08300	252.0	12.0
18	53	0.15000	456.0	6.7
20		0.30000	912.0	3.3
21	56	0.47000	1430.0	2.1

7. COMPUTER MODELS TO DETERMINE THE THERMAL INJURY FROM EXPERIMENTAL DATA

Since the availability of adequate information on the thermal tolerances and damage of living tissue due to heating, computer models have been developed for the analysis of experimental data. In 1960, Stoll [23] first developed an algorithm to evaluate the measurements of the changes in surface temperature with time throughout heating and cooling of the skin by thermal irradiation. From these measured surface temperatures (T_s), Stoll calculated the tissue temperature at the basal layer (approximately 80 μm deep, where the base of the blister forms) using Equation (8). Typical measured temperature histories at the skin surface and those computed at 80 μm are shown in Figure 15 for two irradiances with durations just sufficient to produce minimal blistering within 24 hours. The damage rate ($d\Omega/dt$) was then determined by using the radiative heating curve in Figure 13. This curve is represented by:

$$\log \frac{d\Omega}{dt} = \text{slope} \times T_x + \log (\text{intercept}) \qquad (33)$$

where slope = 0.42 for $T_x < 50°C$

= 0.16 for $T_x > 50°C$

T_x = tissue temperature at 80 μm, °C.

Figure 16 shows the plots of the damage rate vs. the time at which the basal layer temperature occurred for the two irradiances. To calculate the total damage (Ω) including the damage during heating as well as cooling, Stoll integrated the curves shown in Figure 16 over the periods the temperatures at the basal layer remained above 44°C (the injurious level). Applying the trapezoidal rule for integration, the total damage can be expressed as:

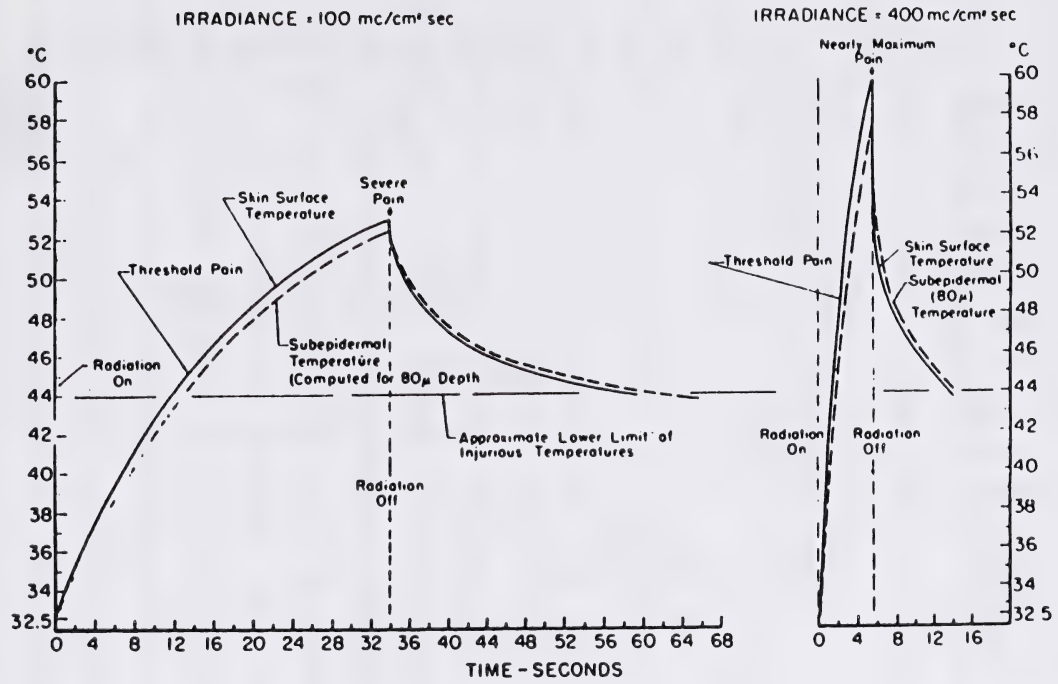

Figure 15 Temperatures at the Surface and Those Calculated at 80 μm During Heating and Cooling of the Skin by Thermal Radiation. From Stoll and Chianta [2].

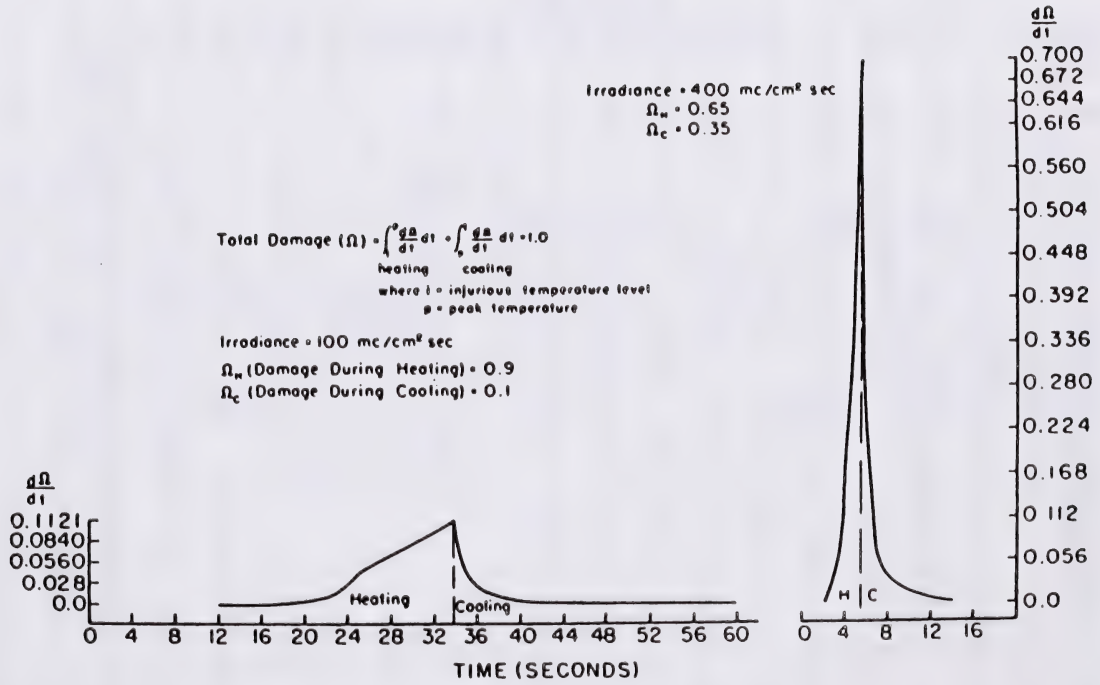

Figure 16 Damage Rate Versus the Time at Which the Basal Layer Temperature Occurred. From Stoll and Chianta [2]

$$\Omega = \int_{i}^{p} \frac{d\Omega}{dt}\,dt + \int_{p}^{i_r} \frac{d\Omega}{dt}\,dt$$

$$= \frac{\Delta t}{2}\left[\dot{\Omega}_o + 2\dot{\Omega}_1 + 2\dot{\Omega}_2 + \ldots + 2\dot{\Omega}_{(N-1)} + \dot{\Omega}_N\right] \qquad (34)$$

where i = time at which the injurious temperature level (44°C) is reached, sec
p = time at which the exposure is removed, sec
i_r = time at which temperature returns to 44°C, sec
Δt = time interval for numerical integration, sec
$\dot{\Omega}_j$ = damage rate $d\Omega/dt$ at the j^{th} grid point, sec^{-1}
N = total number of grid points including the heating and cooling phases

The above procedure developed by Stoll [23] requires direct measurement of the skin surface temperature during irradiation. Weaver and Stoll [10] modified the method to eliminate the measurements of skin temperature. Instead, they measured the radiation intensity and time (a much easier task as mentioned by them) and calculated the basal layer temperature using Equation (11). They also considered the variations of thermal conductivity of the skin with the temperature of the basal layer. By assuming $\rho c \approx 1$ $cal/cm^3 \cdot °C$ so that $\alpha \approx k$, the conductivity solved by them has been presented in Figure 8 in Chapter 4. Since little variation was observed at temperatures above 44°C, they assumed a constant value for the thermal conductivity during the heating phases, that is the average value for temperatures between 44°C and the peak temperature. During the cooling phases, it was found that a constant conductivity failed to represent the temperature drop. Weaver and Stoll, then, established an algorithm to estimate the conductivity during cooling at each temperature point corresponding to each of the grid points on the time scale after the exposure was removed. This algorithm is:

$$\sqrt{k_j} = \sqrt{k_{j-1}} - 10^{-4}, \quad j = 2, 3, \ldots n \tag{35}$$

where k_1 = The average conductivity during cooling for temperatures greater than 44°C and less than the peak temperature, cal/cm sec°C

n = number of grid points after the peak temperature point

Thus, the square root of the conductivity at the j^{th} time-temperature point was estimated by subtracting a constant value of 10^{-4} $(\text{cal/cm sec°C})^{1/2}$ from that at the previous point. This procedure was repeated for each successive point until the point at which the tissue temperature at 80 μm deep decreases back to 44°C. Figure 17 shows the plots of the theoretical conductivity as predicted by this method. Some of the experimental conductivity curves from Figure 8 are also included for comparison. This theoretical function of conductivity was found to be capable of representing the experimental time-temperature histories at various levels of radiation. A comparison of the experimental and the calculated theoretical time-temperature histories for a level of radiation 0.4 cal/cm^2 sec is given in Figure 18.

Once the time-temperature history at the basal layer was obtained, Weaver and Stoll computed the damage rate by using Equation (25). The constant P and the activation energy divided by the gas constant $\Delta E/R$ were determined by using Equation (33) or Figure 13. Values of $d\Omega/dt$ and T_x from Equation (33) were substituted into Equation (25) which yielded solutions for P and $\Delta E/R$. These values are:

$$\left.\begin{aligned} P &= 2.185 \times 10^{124} \text{ sec}^{-1} \\ \Delta E/R &= 93534.9 \text{ K} \end{aligned}\right\} \quad \text{for } 44°C \leq T_x < 50°C$$

and

$$\left.\begin{aligned} P &= 1.8230 \times 10^{51} \text{ sec}^{-1} \\ \Delta E/R &= 39109.8 \text{ K} \end{aligned}\right\} \quad \text{for } T_x \geq 50°C$$

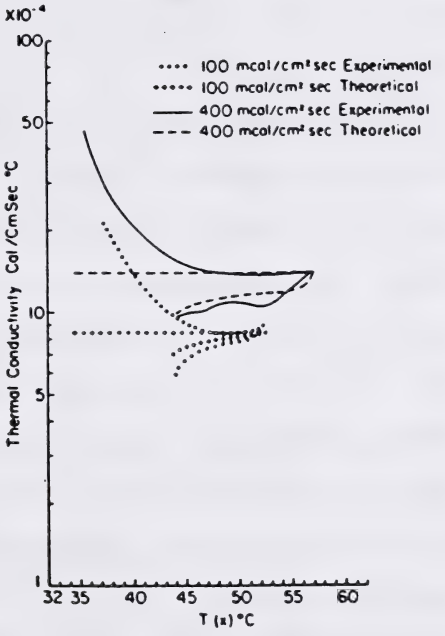

Figure 17 Experimental and Theoretical Thermal Conductivity of Skin versus Tissue Temperature. From Weaver and Stoll [10]

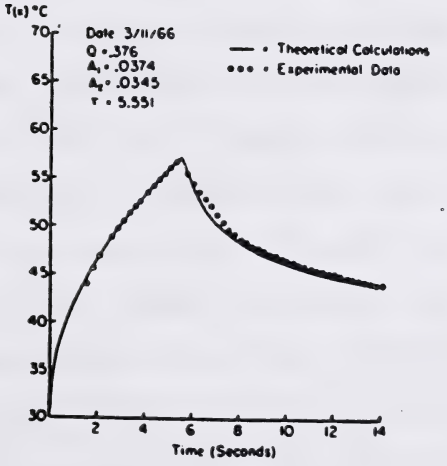

Figure 18 Experimental and Theoretical Time-Temperature History at the Basal Layer for an Irradiance of 0.4 cal/cm^{2}sec. From Weaver and Stoll [10].

Similarly, upon integration of the damage rate by the trapezoidal rule gives the total damage.

The exposure times (τ) required to produce minimal blistering within 24 hours for irradiation between 0.1 and 0.4 cal/cm^{2}sec have been measured [12] and the changes in thermal conductivity with temperature during the heating and cooling phases for this range of irradiation have also been predicted [10]. In order to obtain the same information for irradiation above 0.4 cal/cm^{2}sec, Weaver and Stoll plotted the exposure time (τ), the thermal conductivity during heating, and that during cooling against the radiation with extrapolations to the higher levels (Figures 19 and 20). The effective radiation indicated in Figures 19 and 20 is the absorbed radiation by the skin. In Figure 20 the value of the thermal conductivity during heating for any given radiation level is the constant value used to compute the temperature rise at every time-temperature point. However, the conductivity during cooling is k_1, the conductivity at the first time-temperature point after the peak temperature. From the information given in Figures 19 and 20, the tissue temperature at 80 μm deep when $t = \tau$ (peak T_X), the total time from $t = 0$ to the time at which the tissue temperature falls below 44°C, the damage during heating (Ω_H), the damage during cooling (Ω_C), and the total damage ($\Omega_T = \Omega_H + \Omega_C$) up to a radiation level of 3.0 cal/cm^{2}sec can be calculated by means of the numerical procedure developed by Weaver and Stoll. These results are summarized in Table 14 in which Q is the effective radiation; Δt is the time interval used to calculate Ω; and A_1 and A_2 are the square root of the conductivity shown in Figure 20 during heating and cooling respectively.

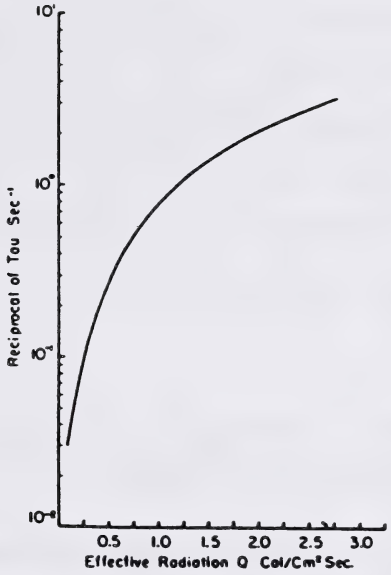

Figure 19 Reciprocal of τ versus Radiation Level. From Weaver and Stoll [10]

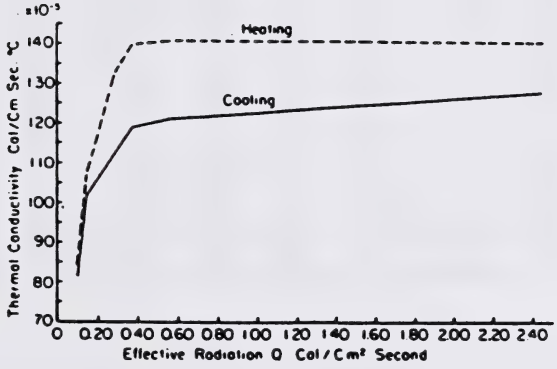

Figure 20 Thermal Conductivity versus Radiation Level. From Weaver and Stoll [10]

As seen, $\Omega_T \simeq 1$ for all the exposures shown in Table 14. Therefore, they are the threshold exposures just sufficient to cause minimal blistering. Also, it is noted that a larger portion of the tissue damage is done after the exposure ceased at the higher radiation levels. In this case, the total amount of heat required to produce minimal blistering is lesser at the higher radiation levels than at the lower levels. The damage incurred during cooling can be minimized by prompt application of ice to the exposed area.

Table 14 Characteristics of Time-Temperature Histories of Skin Exposed to Thermal Radiation Just Sufficient to Cause Minimal Blistering. From Weaver and Stoll [10].

Q (cal/cm²-sec)	τ (sec)	Total Time (sec)	Δt (sec)	Peak T_s (°C)	Heating A1 (cal/cm²-sec-°C)^½	Cooling A2 (cal/cm²-sec-°C)^½	Ω_H	Ω_C	Ω_T
0.094	33.470	52.47	1.0000	52.78	0.0290	0.0283	0.8680	0.1115	0.9795
0.141	21.090	35.76	0.6667	53.81	0.0327	0.0319	0.8251	0.1353	0.9604
0.282	8.300	18.63	0.3333	56.02	0.0364	0.0336	0.7354	0.2428	0.9782
0.376	5.550	13.80	0.2500	57.13	0.0374	0.0345	0.7268	0.2573	0.9841
0.564	3.000	8.50	0.1667	58.80	0.0375	0.0348	0.6982	0.2639	0.9621
0.752	1.950	6.20	0.1250	60.00	0.0375	0.0349	0.6820	0.2796	0.9616
0.940	1.410	5.01	0.1000	61.01	0.0375	0.0350	0.6910	0.3056	0.9965
1.128	1.080	4.16	0.0833	61.72	0.0375	0.0351	0.6705	0.3200	0.9905
1.316	0.862	3.56	0.0710	62.25	0.0375	0.0352	0.6435	0.3301	0.9736
1.504	0.713	3.17	0.0630	62.77	0.0375	0.0353	0.6326	0.3436	0.9762
1.692	0.603	2.84	0.0560	63.15	0.0375	0.0354	0.6099	0.3545	0.9644
1.880	0.522	2.62	0.0500	63.56	0.0375	0.0355	0.6034	0.3778	0.9811
2.068	0.459	2.44	0.0450	63.93	0.0375	0.0356	0.5978	0.4032	1.0010
2.256	0.409	2.30	0.0420	64.28	0.0375	0.0357	0.6011	0.4244	1.0255
2.444	0.367	2.19	0.0380	64.52	0.0375	0.0358	0.5802	0.4446	1.0248
2.632	0.333	2.06	0.0360	64.78	0.0375	0.0359	0.5779	0.4615	1.0394
2.820	0.305	1.95	0.0330	64.91	0.0375	0.0360	0.5456	0.4716	1.0172

In the 1970's, skin damage due to laser irradiation became a topical subject. Consequently, computer models that are suitable for analyzing the complex conditions of burn injury produced by a laser were developed. These models are capable of simulating the effects of blood flow, metabolism, and temporal and multi-dimensional spatial variations in heating [18, 24]. In the present review, laser irradiation of tissue will not be covered.

8. SUMMARY

The previous sections have described the mathematical and physical analysis of the physiological response of skin to burns. Methods to predict thermal damage to tissue have also been discussed.

Under normal conditions, the skin temperature is about 33°C. When the skin is exposed to a heat flux, the skin temperature increases. The increase of skin temperature can be described by the standard one-dimensional heat conduction equation. When the temperature of the skin is elevated to about 44°C, the pain receptors in the skin will give warning of the potentially harmful conditions. At about the same temperature, tissue damage begins. The rate of damage can be represented by a rate process equation which is a function of the skin temperature only. An arbitrary function Ω is used in this equation to describe the amount of damage. When $\Omega = 1$, the threshold of second degree burn occurs. Second degree burn is defined as the damage that indicates complete destruction of the epidermis without a significant degree of injury to the dermis. At this threshold burn, the attachment between epidermis and dermis is impaired. The amount of edema fluid that accumulated under the epidermis is usually sufficient to form a blister. Thus blistering normally indicates destruction of epidermis. When $\Omega > 1$, damages are irreversible.

Like the rate of tissue damage, pain depends only on the temperature to which the skin is raised. Maximum perceptible pain occurs at around 60 to 70°C. While the amount of damage (degree burns) and blistering are dependent on both the temperature and time. The temperature and time required to produce a certian degree of damage are inversely related and can be described by a simple exponential function. In general, when the

temperature of the skin is maintained at 44°C (the minimum injurious level), an exposure of about 6 hours is required before the occurrence of a second degree burn. At temperatures above 70°C, a second degree burn can be produced in less than 1 second.

The occurrence of pain and tissue damage during a burn are mainly due to the thermal denaturation of cellular proteins which have an activation energy of roughly 150,000 cal/mole.

REFERENCES

1. Anthony, C.P. and Thibodeau, G.A., "Textbook of Anatomy and Physiology", 10th edition, The C.V. Mosby Company, St. Louis, 1979.

2. Stoll, A.M. and Chianta, M.A., Heat Transfer Through Fabrics as Related to Thermal Injury, Transactions of the New York Academy of Science, Vol. 33, p. 649, 1971.

3. Gardner, W.D. and Osburn, W.A., "Anatomy of the Human Body", W.B. Saunders Company, Philadelphia, 1978.

4. Southwood, W.F.W., The Thickness of the Skin, Plastic and Reconstructive Surgery, Vol. 15, p. 423, 1955.

5. Henriques, F.C. Jr. and Moritz, A.R., Studies of Thermal Injury: I. The Conduction of Heat to and Through Skin and the Temperatures Attained Therein. A Theoretical and an Experimental Investigation, American Journal of Pathology, Vol. 23, p. 531, 1947.

6. Buettner, K., Effects of Extreme Heat and Cold on Human Skin: I. Analysis of Temperature Changes Caused by Different Kinds of Heat Application, Journal of Applied Physiology, Vol. 3, p. 691, 1951.

7. Schneider, P.J., "Conduction Heat Transfer", Addison-Wesley Publishing Company, Inc., Reading, Massachusetts, 1955.

8. Holman, J.P., "Heat Transfer", 4th Edition, McGraw-Hill, Inc., New York, 1976.

9. Kreyszig, E., "Advanced Engineering Mathematics", 3rd Edition, John Wiley and Sons, Inc., New York, 1972.

10. Weaver, J.A. and Stoll, A.M., Mathematical Model of Skin Exposed to Thermal Radiation, Aerospace Medicine, Vol. 40, p. 24, 1969.

11. Lipkin, M. and Hardy, J.D., Measurement of Some Thermal Properties of Human Tissues, Journal of Applied Physiology, Vol. 7, p. 212, 1954.

12. Stoll, A.M. and Greene, L.C., Relationship between Pain and Tissue Damage Due to Thermal Radiation, Journal of Applied Physiology, Vol. 14, p. 373, 1959.

13. Buettner, K., Effects of Extreme Heat and Cold on Human Skin: II. Surface Temperature, Pain and Heat Conductivity in Experiments with Radiant Heat, Journal of Applied Physiology, Vol. 3, p. 703, 1951.

14. Effects of Atomic Weapons, Washington, D.C.: U.S. Government Printing Office, 1950.

15. Moritz, A.R., Studies of Thermal Injury: III. The Pathology and Pathogenesis of Cutaneous Burns, An Experimental Study. American Journal of Pathology, Vol. 23, p. 915, 1947.

16. Moritz, A.R. and Henriques, F.C., Studies of Thermal Injury: II. The Relative Importance of Time and Surface Temperature in the Causation of Cutaneous Burns, American Journal of Pathology, Vol. 23, p. 695, 1947.

17. Hardy, J.D., Wolff, H.G. and Goodell, H., Studies on Pain: Discrimination of Differences in Intensity of a Pain Stimulus as a Basis of a Scale of Pain Intensity, Journal of Clinical Investigation, Vol. 26, pp. 1152, 1947.

18. Diller, K.R., Analysis of Skin Burns, in Shitzer, A. and Eberhart, R.C., "Heat Transfer in Medicine and Biology", Plenum Press, New York, Vol. 2, Chapter 18, 1985.

19. Hardy, J.D., Jacobs, I. and Meixner, M.D., Thresholds of Pain and Reflex Contraction as Related to Noxious Stimulation, Journal of Applied Physiology, Vol. 5, p. 725, 1953.

20. Stoll, A.M. and Chianta, M.A., Method and Rating System for Evaluation of Thermal Protection, Aerospace Medicine, Vol. 40, p. 1232, 1969.

21. Henriques, F.C., Studies of Thermal Injury: V. The Predictability and the Significance of Thermally Induced Rate Processes Leading to Irreversible Epidermal Injury, Archives of Pathology, Vol. 43, p. 489, 1947.

22. Glasstone, S., Laidler, K.J. and Eyring, H., "The Theory of Rate Processes", McGraw-Hill Book Company, Inc., New York, 1941.

23. Stoll, A.M., A Computer Solution for Determination of Thermal Tissue Damage Integrals from Experimental Data, IRE Transactions on Medical Electronics, ME-7, p. 355, 1960.

24. Welch, A.J., Laser Irradiation of Tissue, in Shitzer, A. and Eberhart, R.C., "Heat Transfer in Medicine and Biology", Plenum Press, New York, Vol. 2, Chapter 19, 1985.